

A Dissertation
On
Effect of Processing Parameters on the Hardness and
Sliding Wear Behaviour of Sintered Cu-CNT Composite

Submitted in the partial fulfilment

for the Degree of

Master of Engineering

in

CAD/CAM

Submitted by:

Gaganpreet Singh Hunjan

Roll No. 801584004

Under the supervision of:

Dr. Hiralal Bhowmick

Assistant Professor

Mechanical Engineering Department

Dr. Vineet Srivastava

Assistant Professor

Mechanical Engineering Department

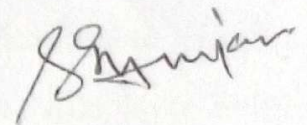


MECHANICAL ENGINEERING DEPARTMENT
THAPAR UNIVERSITY
PATIALA-147004, PUNJAB, INDIA
July 2017

CERTIFICATE

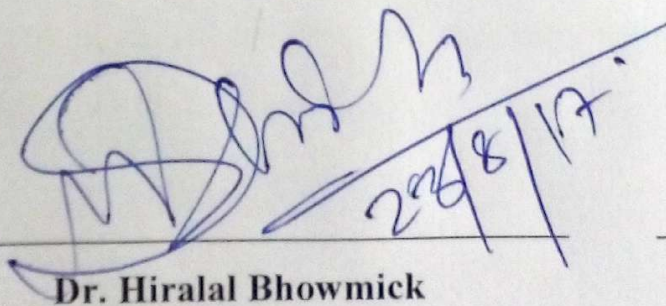
I hereby declare that the thesis entitled “**Effect of Processing Parameters on the Hardness and Sliding Wear Behaviour of Sintered Cu-CNT Composite**” is an authentic record of my study carried out as requirements for the award of the degree of **Master of Engineering in CAD CAM & Robotics** at **Thapar University, Patiala** under the supervision of Dr. Hiralal Bhowmick & Dr. Vineet Srivastava, Assistant Professor, Mechanical Engineering Department, Thapar University, Patiala during July, 2016 to July, 2017. The matter embodied in this report has not been submitted to any other university or institute for the award of any degree.

Date: 23/08/2017



Gaganpreet Singh Hunjan

It is certified that the above statement made by the student is correct to the best of our knowledge and belief.

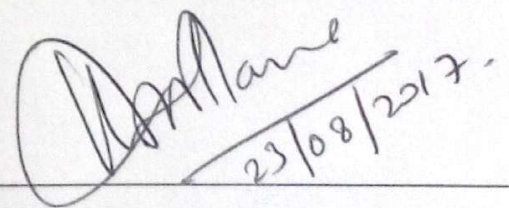


23/08/17.

Dr. Hiralal Bhowmick

Assistant Professor

Mechanical Engineering Department



23/08/2017.

Dr. Vineet Srivastava

Assistant Professor

Mechanical Engineering Department

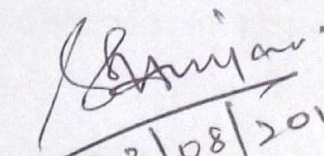
Acknowledgement

I would like to acknowledge my mentors **Dr. Hiralal Bhowmick** and **Dr. Vineet Srivastava**, **Assistant Professors, Department of Mechanical Engineering, Thapar University, Patiala**, for their constructive suggestions and positive guidance in the thesis work. I am really grateful to spend many opportune moments under their outstanding management which inspired me a lot for carried out my research work.

I am greatly thankful to **Dr. S. K. Mohapatra**, **Sr. Professor and Head, Department of Mechanical Engineering** for his encouragement and inspiration for execution of the seminar work. I am also very thankful to the entire faculty and staff members of Mechanical Engineering Department for their direct- indirect help and cooperation.

Now, I would like to acknowledge **Mr. Kulwinder Singh**, **Mr. Arminder Singh** and **Mr. Harpreet Singh**, **Research Scholars, Thapar University, Patiala**, who have helped me at their best in various sections of my research work. Also, I would like to thank my friends especially **Mr. Jaspreet Singh**, **Mr. Amardeep Singh** and **Mr. Kamaldeep Sharma** who always backed up and motivated me throughout my complete research work,

In the end, I wish to express my deep sense of gratitude to my family, for supporting and encouraging me at every step of work. It is their blessings, which has given me the courage, confidence and zeal for hard work.


23/08/2017

Abstract

Copper has high thermal conductivity, superior corrosion and oxidation resistance, while CNT enhances strength and wear resistance properties to the matrix. There are several potential applications for these composites such as break shoes, cylinder liners as well as piston rings where high strength, hardness and wear resistance as well as good thermal conductivity are some of the desired properties required for the developed materials. Looking at its potential outcome, in the present research, an attempt is made to develop Cu-CNT composite with optimized process parameters for improved hardness and wear characteristics. In the present investigation, the composites are fabricated via powder metallurgy route. Copper metal in powdered form with 99.5 per cent purity and multi walled CNT are used as for the matrix and reinforcement. In the present study three processing parameters are considered namely ultrasonic agitation energy, volume percentage inclusion of reinforcement with respect to matrix and the sintering temperature which predominantly govern the tribological properties. The influences of these processing parameters on the hardness and wear resistance of the fabricated composites are then investigated in details. The study also includes the estimation of elastic properties of the fabricated composites using the mathematical model proposed and simulation of wear depth using general purpose FEA software package ANSYS Mechanical APDL, which is then followed by the experimental validation. From the study it is observed that the sintering temperature and amount of reinforcements has immense influence on the mechanical and wear properties of the fabricated composite. The variation of sonication energy for the dispersion of the particles for mixing is not having much significance for the same. An inverse correlation of wear depth with the hardness of the material could also be observed. The simulation data is found to be well in agreement with the experimental observations.

Key words :Wear, Nano-composite, FEM, Powder Metallurgy

Table of Contents

Certificate.....	i
Acknowledgement	ii
Abstract.....	iii
List of Figures	vii
List of Tables	ix
Nomenclature and List of Abbreviations	x
Chapter 1 Introduction.....	1
1.1 Introduction	1
1.2 Need of Wear Modelling.....	1
1.3 Approaches for Finite Element Wear modelling.....	2
1.4 Composite Material	2
1.5 Types of Composite Material	3
1.5.1 Metal Matrix Composite (MMC).....	3
1.5.2 Ceramic Matrix Composite (CMC)	3
1.5.3 Polymer Matrix Composite (PMC).....	3
1.6 Applications of Cu-CNT composites	4
1.7 Processing techniques for fabrication of Cu-CNT composites	5
1.7.1 Powder metallurgy	5
1.7.2 Mechanical alloying.....	6
1.7.3 Squeeze Casting	6
1.8 Summary	7
Chapter 2 Literature Survey	8
2.1 Introduction	8
2.2 Literature Review on the Fabrication and Characterization of Cu-CNT composites	8

2.3	Literature Review on the Wear Modelling.....	15
2.4	Summary of Literature review and Identification of Research gaps.....	17
Chapter 3 Research Objectives and Methodology		18
3.1.	Introduction	18
3.2.	Problem formulation and Setting up Research Objectives.....	18
3.3.	Material selection	19
3.3.1.	Matrix.....	19
3.3.2.	Reinforcement.....	19
3.4.	Design of experiments.....	20
3.5.	Experimental Facility Used For Composite Fabrication and Sample Preparation....	21
3.5.1.	Weighing Balance	21
3.5.2.	Ultrasonic agitator.....	21
3.5.3.	Molecular level Mixing.....	22
3.5.4.	Ball milling	22
3.5.5.	Cold Compression.....	22
3.5.6.	Sintering	23
3.5.7.	Facing.....	23
3.5.8.	Disk Polisher.....	24
3.6.	Experimental Facility Used For Tribology Study	24
3.7.	Experimental Facility Used For Mechanical and Metallurgical Investigation	25
3.7.1.	Hardness.....	25
3.7.2.	Field Emission Scanning Electron Microscope and EDX	26
3.8.	Mathematical Calculation of Elastic Properties of Nano composite.....	27
3.9.	Modelling of Wear Depth	27
Chapter 4 Results and Discussion		31
4.1.	Introduction	31
4.2.	Morphological and Metallurgical characterization of fabricated samples	31

4.2.1. FESEM Micrographs	31
4.2.2. Energy Dispersive X-Ray Spectroscopy.....	33
4.3. Micro-hardness vs. Wear Depth.....	35
4.4. Worn Out Pin Surface Analysis	38
4.5. Disc Wear Track Analysis.....	41
4.6. Finite Element Simulation of Wear.....	42
4.7. Summary	46
Chapter 5 Conclusion	47
5.1. Conclusion.....	47
5.2. Recommendation for future works.....	48
References.....	49
Appendix A: Formulae used for the calculation of various elastic constants.....	52

List of Figures

Figure 2.1:	Variation of friction coefficient and wear rate with sliding speed	9
Figure 2.2:	Variation of density with volume of reinforcement	9
Figure 2.3:	Strain vs. Stress for pure copper and copper-CNT composite	10
Figure 2.4:	Wear loss and Friction coefficient vs. Reinforcement volume	11
Figure 2.5:	Effect of yield strength dependence on reinforcement content	11
Figure 3.1:	Weighing Balance [Photo Courtesy: Thapar University, Patiala]	21
Figure 3.2:	Ultrasonicator [Photo Courtesy: Thapar University, Patiala]	22
Figure 3.3:	Manual Hydraulic Press [Photo Courtesy: Thapar University, Patiala]	23
Figure 3.4:	(a)Tubular Furnace[Photo Courtesy: Thapar University, Patiala]	23
Figure 3.5:	Numerically Controlable Lathe Machine [Photo Courtesy: Thapar University, Patiala]	24
Figure 3.6:	Wear testing apparatus[Photo Courtesy: Thapar University, Patiala]	25
Figure 3.7:	Micro Hardness Tester [Photo Courtesy: Thapar University, Patiala]	25
Figure 3.8:	FESEM Preprocessing [Courtesy: Panjab University, Chandigarh]	26
Figure 3.9:	Laboratory Setup of FESEM [Courtesy: Panjab University, Chandigarh]	26
Figure 4.1:	SEM Micrographs of specimens with hardness values with CNT as marked (a) 120 VHN (b) 116 VHN (c) 118 VHN	32
Figure 4.2:	EDS Results of specimens with hardness values 120 VHN	33
Figure 4.3:	EDS Results specimens with hardness values 116 VHN	34
Figure 4.4:	EDS Results specimens with hardness values 118 VHN	34
Figure 4.5:	Effect of Sonication Energy and % CNT on (a) Microhardness and (b) Wear depth at 750°C	36
Figure 4.6:	Effect of Sonication Energy and % CNT on (a) Microhardness and (b) Wear depth at 850°C	36
Figure 4.7:	Effect of Sonication Energy and % CNT on (a) Microhardness and (b) Wear depth at 950°C	37
Figure 4.8:	Effect of Sintering Temperature on (a) Microhardness and (b) Wear depth for particles mixing at 50% sonication energy	37
Figure 4.9:	Scatter plot of wear depth and Vicker hardness	38
Figure 4.10:	Pins Worn Surface (a) 3% CNT (b) 8% CNT (c) 12% CNT	40
Figure 4.11:	Wear track on the counter disc	42
Figure 4.12:	Mesh Generation for Pin on Disk apparatus	43
Figure 4.13:	Simulated and experimental wear depth obtained for specimens (a)120 VHN	44

(b)92 VHN (c)73 VHN

Figure 4.14: (a)Typical wear Depth plot depicting variation in slope with time (b) Typical friction plot 44

Figure 4.15: Simulated and experimental wear depth obtained for hardness 116 VHN and $K=1.4 \times 10^{-5}$ 45

Figure 4.16: Surface profile of Composite Pin for wear simulation (a) 10 sec after start (b) 440 Sec 45

List of Tables

Table 3.1	Composition of Metallic Copper	19
Table 3.2	Properties of Multi walled Carbon Nanotubes	20
Table 3.3	Processing parameters selected for composite specimen preparation	20
Table 4.1	Elemental composition of the fabricated samples with hardness values 120 VHN	33
Table 4.2	Elemental composition of the fabricated samples with hardness values 116 VHN	34
Table 4.3	Elemental composition of the fabricated samples with hardness values 118 VHN	34
Table 4.4	Hardness and Wear depth for various composite samples	35
Table 4.5	Elemental composition of Pin Worn Surface (8% CNT)	40
Table 4.6	Elemental composition of Pin Worn Surface (3% CNT)	41
Table 4.7	EDS results of counter disk subjected to pins with hardness values (a)120VHN (b)118 VHN	42

Nomenclature and List of Abbreviations

ASTM	American Society for Testing and Materials
MWCNT	Multi Walled Carbon Nano-tubes
FESEM	Field Emission Scanning Electron Microscopy
FEA	Finite Element Analysis
μ	Coefficient of Friction
K	Coefficient of Wear
c_r	Concentration of Reinforcements
n_r	Uniaxial Tension Modulus of reinforcement
m_r	Cross Modulus of reinforcement
k	Bulk Modulus
p_r	Shear Modulus

Chapter 1 Introduction

1.1 Introduction

Wear is an unavoidable phenomenon in real world whether it is in reference to machining or in reference to a component used as a functional part. Wear is the removal of material in terms of mass from the surfaces of objects in interaction with each other. In contrast to the machining, wear is undesirable which in most of the cases is responsible for the reduction in the strength of materials and reduction of the service life of the component or product. It is not merely the dislocation or deformation of that material to some different part of the object. Wear of components is often a key factor influencing the product service life and due to that wear prediction is an important part of engineering. Basically wear can be divided into two major subcategories, namely, wear dominated by mechanical behaviour of given materials which includes wear mechanisms such as asperity deformation, ploughing, adhesive wear, abrasive wear, fretting wear and wear dominated by chemical behaviour of the materials incorporating the mechanisms such as solution wear, oxidation wear, diffusion wear, wear by melting of the surface layer[1].

1.2 Need of Wear Modelling

The most accurate knowledge of tribological behaviour of any friction pair can be achieved by actually carrying out the wear experiments. However, it is a destructive process so other designs alternatives are in demand for wear evaluation. There exist different statistical and analytical ways to model the particular behaviour of a material however to an extents these approaches are also destructive in nature for the collection of data required to calculate statistics. Finite element analysis is one such non-destructive process. In the past, wear calculation between surfaces was not a concern in finite element analysis since this method was seen majorly for calculation of loads needed for design analysis and after determining load distribution it was used to perform detailed component evaluation of structure. Even if fatigue was calculated to predict the life of structure, the effects of wear were assumed to be small and thus neglected. Over the time, the mechanics and effect of wear are being better understood and its calculation and reduction are becoming critical too. Also, the increasingly

complex geometries for tribological pairs is heading to consider use of FE analysis for calculation of wear.

1.3 Approaches for Finite Element Wear modelling

Basically there exist three forms of surface interaction which can cause wear namely sliding wear, fretting wear and erosion wear. However, in the following chapters dry sliding wear is kept under scope. Also, there are number of variables which have significant effect on dry sliding wear such as surface geometry and finishing, hardness of the material, microstructure of material and the pressure on the component. Modelling of the wear can be done in two possible ways. First, in which the minute details such as surface finish and the interaction behaviour should be included in the model so that each removed element exactly simulates the wear mechanisms such as ploughing. Therefore, it is required to keep each element as the size of particle of the material and molecules. This in turn requires large amount of calculations time as well as the suitable protocol for its actuation. Second, in which the macro scale approach is used by keeping the element size much larger than the expected changes due to wear such that the calculations are performed within the elements [2]. Furthermore, if a heterogeneous surface interaction is to be inspected, the challenge grows manifolds like the ones encountered during composite material FEA, the particular properties required in certain applications [3]. Keeping in view the complexities of the modelling we will be analysing using the second approach in the next chapters.

1.4 Composite Material

A composite material has two or more constituent materials with significantly different physical or chemical properties. However, the characteristics of the fabricated composite are different from the individual constituent. Unlike in alloys, the individual constituent in composites remains separate and distinct within the finished structure. The primary material which is called matrix acts as the continuous phase such as metals, polymers while the reinforcements such as fibres, particles, and whiskers acts as discontinuous phase. The protruding reinforcements usually carry the major fraction of load, whereas the matrix enables the load transfer by holding the reinforcements together.

1.5 Types of Composite Material

1.5.1 Metal Matrix Composite (MMC)

In a metal matrix composite the primary matrix material consists of a metal, whereas, the secondary constituent may be another metal or different material such as fiber, particulate, whisker or organic compound. If more than two materials are present in the fabricated product then it is known as hybrid composite. MMCs are made by dispersion of a reinforcing material into matrix. The reinforcement surface can either be coated or not depending on the wettability characteristics required for the particles. For example, carbon and its derivatives can be used in copper matrix to develop composites having low density and high strength. Sometimes to improve the wettability of reinforcement; the particles are coated with nickel before the mixing process. When compared to monolithic materials, MMCs are better due to better strength to density ratio, superior fatigue resistance, better properties at elevated temperatures, better stiffness to density ratio, lower creep rate, etc.

1.5.2 Ceramic Matrix Composite (CMC)

Ceramic matrix composites are the materials in which more than one distinct phases of ceramic are intentionally added to the other in order to improve some properties that are not possessed by the monolithic material. In ceramic matrix composite, base ceramic matrix is reinforced with either continuous fibres or reinforcements such as particles, whiskers or cut fibres. For example carbon, glasses, glass ceramics, oxides and non-oxides are the generally used reinforcements in ceramic matrices. The primary aim of reinforcement is to provide toughness to an otherwise brittle matrix. The processing temperatures for ceramic matrix composites are extremely high as compared to metal or polymer matrix composites which in turn lead to difficult and expensive processing.

1.5.3 Polymer Matrix Composite (PMC)

PMC has organic polymers as matrix and fibres, whiskers, etc as reinforcement. Generally, in these composites fibers are the main load bearing components due to their high strength and modulus. Matrix material should possess high adhesion properties for appropriate bonding with the reinforcements as well as to uniformly distribute the applied load by transferring the loads to fibre. Also, the matrix material

is chosen by the desired properties for the selected application. The PMC materials may be produced in the various finished structure such as thermosetting or thermoplastic resin-based, single component PMC materials or polymer blends matrix composite materials.

However, unless specifically required, MMCs are more popular as compared to PMCs due the superior properties of MMCs as compared to PMCs such as higher temperature adaptability, better resistance to radiation, negligible moisture absorption, better transverse stiffness and strength and excellent resistance to fire.

1.6 Applications of Cu-CNT composites

Carbon nanotube (CNT) has low density, very high strength and stiffness, good electrical properties as well as thermal conductivity. They can be used as reinforcing fibres where high strength and stiffness or high toughness with low weight are major considerations. With the use of the nano sized CNT reinforcements structures can be made thinner and flatter. There are various applications such as structural panels, sports goods, ultra-light weight structures used in space. CNTs are highly effective as a conductive additive because of their good electrical properties, huge aspect ratio and their tendency to possess a three dimensional interconnecting web in molten plastic. Additional applications involving electronic properties are photo voltaic device technologies such as in organic solar cells, electromechanical actuators and LEDs, field effect transistors, optical switches and electromagnetic shields for mobile handsets.

A new application for CNT composites is automobile bumpers [4]. The bumpers are expected to have good mechanical properties and lower weight since due to low density only 1-5 per cent CNT will be needed as compared to at least 30 wt.% of fibreglass.

They have also shown potential application in brake shoes, cylinder liners and piston rings due to the properties desired such as, high wear resistance, high strength and hardness low density, high strength and good thermal conductivity [5].

1.7 Processing techniques for fabrication of Cu-CNT composites

Carbon nanotube reinforced MMCs can be prepared through a variety of fabrication techniques. However, processing of metal-CNT composite has been challenge due to distinct phase of CNT and copper, difference in coefficient of thermal expansion, wettability issues. Poor wettability affects the load transfer and phonon scattering. Agglomeration of CNT causes dispersion problems. Therefore choice of synthesis method plays very important role. Some of the available methods used for synthesis of Cu-CNT are powder metallurgy, casting, molecular-level-mixing, mechanical alloying, electrochemical deposition, etc. The most popular techniques for the production of composite materials are based on casting and powder metallurgy methods[5]. A brief overview of these techniques is described in the following sections.

1.7.1 Powder metallurgy

Powder metallurgy methods are based on classic mixing of matrix and reinforcing powders, followed by cold compaction and sintering. Plastic forming such as extrusion and forging are optional as per requirements of the final product. When a green part is preliminary sintered then cold plastic working is generally performed and hot plastic working is done when only cold compaction is used. Before getting into the core steps of processing it is essential to heat treat the powder i.e. annealing. Annealing the powder helps to softens the particles surface. This process is carried out to get rid of carbon or oxygen content which may be present after the powder production. Another advantage of annealing is it helps to relieve the stress and also removes any oxide layer if present. But most importantly, annealing of the metal powder enhances the compressibility during compaction and green strength of compact due to softened surface layer of metal particles. The heat treated powders are then passed through the various steps to obtain the final composite product such as ball milling or mixing, powder compaction and sintering of green compact.

Ball milling is one of the critical steps in powder metallurgy process to disperse the CNTs into Cu matrix and also to alter the particle size. The various parameters associated with ball milling are Ball to powder ratio (BPR), Rotations per minute (RPM), Milling time duration and type of ball milling machine. In powder

compaction process the composite powder is first transferred to either steel or graphite die and compacted by applying uniaxial force to required dimension. Initially when powder is poured into die particles are arranged in random order with point contact to neighbouring particle. As the force is applied with punch the plastic flow occurs in vicinity of contact. This increases the contact zone and thus centre of particles comes close to each other hence densifying the green compact. After densification the compact obtained are called Green compact. This is followed by the sintering step. Sintering is the process in which green compact is heated in an inert atmosphere up to 70-85% of matrix melting point. During this process the surface of the particles are partially melted and gets bonded with surrounding particles resulting in stronger compact. Volatile impurities are also eliminated during this process. Sintering is generally carried out under Nitrogen or Argon atmosphere to avoid oxidation problems. When sintering is carried out at higher temperature i.e. close to melting temperature of composite grain growth occurs.

1.7.2 Mechanical alloying

Mechanical alloying is now-a-days widely used method for the fabrication of particle or fiber reinforced composites that produce very fine grains, amorphous and magnetic materials. High energy ball mills are used to mix the hard particles to relatively soft metal matrix. The composite powder produced in this way are pressed afterwards and consolidated by hot forging or hot isostatic pressing or cold pressed. This may be followed by sintering and plastic work.

1.7.3 Squeeze Casting

Another production method of composite is squeeze casting where infiltration of porous preheated preforms made by ceramic fibres is subjected to pressure with molten light alloys. There are two types of squeeze casting; direct squeeze casting is used for production of composites characterised by comparatively simpler shapes. Indirect squeeze casting makes possible the production of complex parts. Casting dies for direct casting are simpler and of reasonable prices whereas indirect casting involves more expensive casting dies.

1.8 Summary

In this chapter we have briefly discussed the background and the current needs of Cu-CNT composites as the better substitutes for some of the potential applications where there is growing need of improvements required in material properties as well as the requirement of non-destructive analysis of their behaviour. The current progresses using Cu-CNT in the relevant fields of this thesis work have been discussed in the Chapter 2.

Chapter 2 Literature Survey

2.1 Introduction

There have been significant advancements in the research in the field of composite materials and their fabrication. It is also known that depending upon the size and properties of the particular materials some modifications in the processes are also required which in return show us the enhancements in the required parameters. In this chapter the work that has been done in the fields of fabrication and characterization of CNT reinforced metal matrix composite has been discussed. This review chapter will also discuss some of the works related to FE modelling on mechanical and wear behaviour of metals and the advancements of the same for composites.

2.2 Literature Review on the Fabrication and Characterization of Cu-CNT composites

Yu et al. [6] carried out the study on mechanical strengths and the breaking mechanisms associated with the CNT by tensile loading. Previously, as the strength was predicted to be a function of parameters such as nanotube structure, strain rate and temperature, the method now used was measuring the Stress – Strain response of individual multi walled CNT under tension. A manipulated tool acting as a mechanical loading device inside SEM was developed. They observed that there is no significant dependence of the tensile strength on the diameter of nanotube shell. The measured tensile strengths were in the range of 11-63 GPa. However the relation between Young's Modulus and tensile strength was observed to be inversely proportional varying between 270-950 GPa. The theory for permanent deformation of MWCNT was predicted to be the stress wave generated due to release of elastic energy when breakage at large stresses occur.

Raj Kumar et al. [7] investigated the effects of CNT and sliding velocity on tribological performance of Cu-CNT composite using pin on disk for dry sliding conditions. The composites were fabricated by powder metallurgy technique followed by microwave sintering. It is observed from the Fig. 2.1 that in the case of 10-15 per cent CNT the coefficients of friction as well as the wear rate are minimum. Furthermore, the effect of sliding velocity on the wear rate was observed to be

minimal for both the cases due to surfacing of carbonaceous film on the contact surface. However, the wear rates for 5 and 20 per cent CNT content were found to be higher.

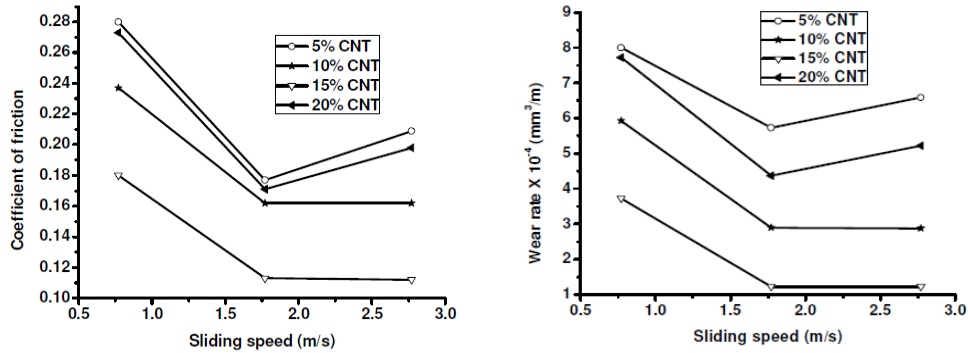


Figure 2.1: Variation of friction coefficient and wear rate with sliding speed [7]

Pham et al. 2011 [8] studied the influence of sintering temperature on the nano-composite density and the effect of CNT volume on its hardness. The observed density (Fig. 2.2) was slightly lesser than the calculated density owing to its porosity with increasing CNT content. Also the hardness of the composites was tested to be best at CNT content of 2 per cent by weight. With further increase in reinforcement the hardness starts to decline due to the agglomeration factor being most significant.

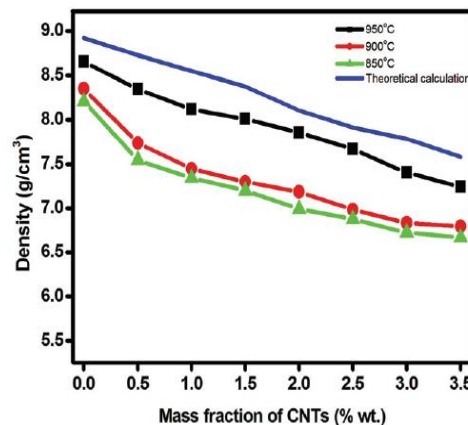


Figure 2.2: Variation of density with volume of reinforcement [8]

Vishlaghi et al. [9] studied the effect of ultrasonic agitation time and ball milling time on the homogeneous dispersion of reinforcement within the matrix. Since the reinforcing particles are very small in size they tend to form clusters due to the Vander-Wall forces of attraction. After CNTs being sonicated for about 20 minutes it was observed that the clusters were broken and the particles dispersion in the matrix

powder was near to homogeneous after ball milling. The mixture was also subjected to different ball to powder ratios to observe the change in particle size at micro level.

Bakshshaei et al. [10] studied the effect of milling time in the formation of homogeneous powder of same average crystal size. They observed that by adding the reinforcement to the mixture in steps, the agglomeration is avoided to a large extent and as they increase the percentage content of reinforcement the average crystal size also decreases significantly.

Li et al. [11] investigated the mechanical properties of CNT reinforced copper compacts which were made by high pressure torsion after being ball milled for 5 hours. It was observed (Fig. 2.3) that although increase in strength generally results in decrease of ductility but the CNT composites showed different trends. The increase in ductility as well as strength has been observed in nanocomposites. The increase in Young's Modulus from 91 to 117 Gpa was also seen with addition of 1 percent CNT by weight. Also as the Stress-Strain graph (Fig. 2.3) suggests, the energy required to failure is 10 percent larger than pure copper.

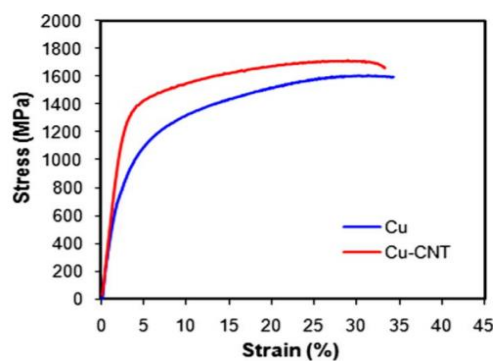


Figure 2.3: Strain vs. Stress for pure copper and copper-CNT composite [11]

Dong et al. [12] studied the effect of nanotubes concentration on the coefficient of friction and wear loss of nanocomposite. A decreasing trend in both the parameters was observed as the CNT content increased as shown in Fig. 2.4. It suggested that presence of nanotubes provides lubrication effect while sliding which results in decrease of wear. However, this happens only upto 10 percent volume of reinforcement as after that the porosity factor of composite starts to dominate than the lubrication effect. It was suggested that the composites with 10-12 percent of CNT and sintered at 850⁰C give the best results.

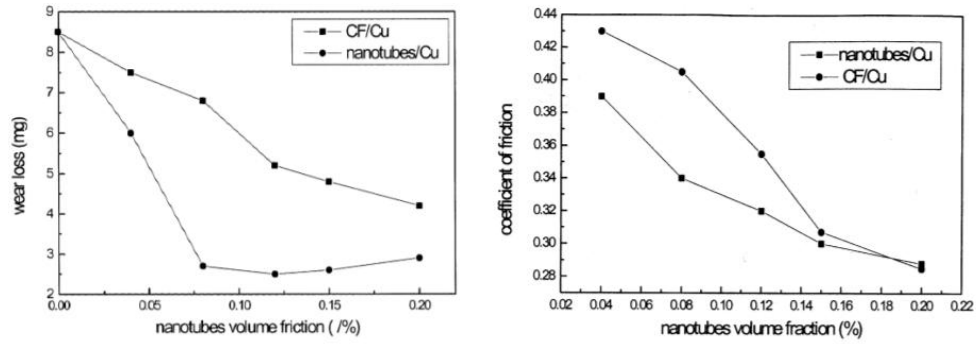


Figure 2.4: Wear loss and Friction coefficient vs. Reinforcement volume [12]

Chu et al. [13] investigated the change in mechanical properties of copper depending on the percentage content of reinforcement. The tensile strength by addition of 10 percent CNT by volume increased by 1.5 times as compared to the pure sample. Furthermore, the yield strength and hardness were also reported to increase by 28-35 percent than their pure counterpart (Fig. 2.5).

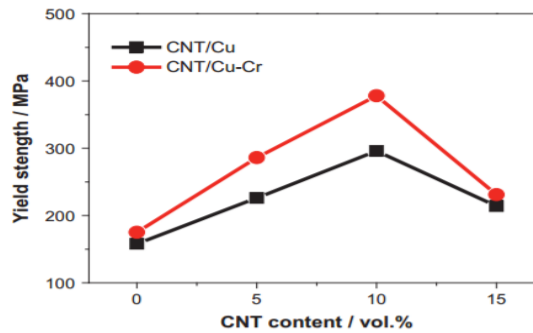


Figure 2.5: Effect of yield strength dependence on reinforcement content [13]

Shi et al. [14] studied the effects of addition of nanotube reinforcements and their agglomeration theoretically using analytical micromechanics models. The composite is treated as an isotropic material since the nanotubes are dispersed homogeneously throughout the matrix. In the case where agglomeration effect is predicted, the reinforcement clusters are considered as in spherical shape inclusion. The study predicts the mechanical characteristics of the composite which can also be used to tailor the required mechanical properties. The theory uses Hill's elastic constants which are dependent on the concentrations of reinforcement, bulk modulus, uniaxial tension modulus, cross modulus and shear modulus in direction normal and parallel to the reinforcement of matrix and reinforcement respectively. The shear modulus in case of homogeneous distribution is taken to be equal in both normal and parallel directions.

A similar behaviour of dependence of wear rate on the percentage of nanoparticles content was observed by Wang et al. [15]. The favourable results of wear rate were attributed to their well dispersion as well as the excellent mechanical properties and also the reversing phenomena while the agglomeration starts taking place with higher reinforcement content. Another thing they observed was that after wear testing the trend of groove formation on the surface of nano composite. With the increasing reinforcement content, the reunited nanoparticles were flaked away during the process. Also, with further increase in CNT volume cracking and spalling was seen on the surface which they attributed to the peeling of agglomerated CNTs which leads to increase in wear loss.

Uddin et al. [16] evaluated the effect of size of matrix phase on mechanical properties and electrical conductivity. They observed that milling the powders for shorter durations does not help in proper embedment of CNTs in the matrix, on the other hand, mixing for prolonged durations promoted cold welding of the metal particles which resulted in lesser CNT embedment in the matrix. To overcome this, they considered the use of reduced particle size which has resulted in better dispersion throughout. This also helped in increase of hardness with decrease in particle size the effect of Hall-Petch. Better dispersion due to reduced particle size helps to provide better interfacial strength which in turn results in increase of composite hardness. Hardness and relative density increased with reduced particle size. The electric conductivity test concluded that CNTs help to improve the hardness of highly conductive but low strength copper metal and improves the electrical conductivity of low conductive but high strength copper alloys.

Yoo et al. [17] studied the difference in effects of a combination of high ratio differential speed rolling (HRDSR) and conventional rolling and it was observed that HRDSR was more effective in increasing the uniformity and orientation of CNT dispersion in copper matrix. In their study, significant amount of CNTs were found on the grain boundaries in case of HRDSR fabricated composites. On the contrary, in the conventionally processed copper composites, CNTs were found poorly dispersed and highly damaged which could have resulted due to high compression imposed during equal speed rolling (ESR). However, they concluded that the poor clustering may be due to the small shear strain imposed during equal speed rolling. It was concluded that grain refinement and dislocation strengthening are the main mechanisms responsible

for ESR and HRDSR composites. They suggested that there is a little contribution of load transfer effect since there was no carbide layer formation at Copper-CNT interface.

Kim et al. [18] used molecular level mixing for the fabrication of nano-composites. The nanoparticles were surface functionalised. The vaporised powders were calcinated into CuO-CNT nano-composite powders followed by reduction into Cu-CNT. It was noted that when CNTs are being functionalised, an electrostatic repulsive force is generated which overcomes Vander Waals force and helps in forming a homogeneous suspension in the solvent. The microstructure of composite was observed to have homogeneous distribution of CNTs throughout. The wear loss decreased by half of the pure metal by addition of CNTs. During the wear process the worn chips of copper metal were formed by peeling of Cu grains near the surface. Unlike this, copper grains were not easily peeled in the nano-composite due to pinning of homogeneously implanted CNTs. Also, another interesting fact they revealed is that the CNT exposed to the surface can as lubricant film owing to its very low coefficient of friction.

Jenei et al. [19] revealed that when the coarse copper powder and CNTs are consolidated by high pressure torsion, the CNTs broke into graphite like fragments during the process. Their hardness measurements suggest that moving away from centre to the periphery within 20% of the radius, the microstructure of composites produced at room temperature starts to be more homogeneous due to extremely high dislocation density. Also, the increase in temperature from room temperature to 373 K showed only a slight increase of grain size. It is concluded that strength in pure Cu as well as Cu-CNT composites is determined majorly by interaction between dislocations.

Alidokht et al. [20] introduced Friction Stir Processing to incorporate reinforcement particles into the matrix to form hybrid composite at the surface. They found that there is more uniform dispersion of reinforcement with the increase in tool rotation rate. The wear resistance of hybrid composite increased with increase in load. The subsurface deformations extended upto depth below the worn surface of hybrid composite. They also observed that relatively smooth signs of abrasion mechanism were exhibited at lower loads, varying between 10 to 25 Newton, for surface hybrid composite produced by tool rotation at higher rpms.

Deng et al. [21] studied the processing and properties of Cu-CNT composites

made by isostatic pressing and hot extrusion techniques. It was observed that nanotubes were distributed homogeneously and acts as bridges across the cracks in matrix while some of them get pulled out on the surface. They found that at the addition of smaller amount of CNT, the density and hardness of composites increases with increasing CNT content. They attributed it to the fact that smaller amounts of reinforcement can fill up the micro voids resulting in density increase. The tensile strength and Young's modulus were found to be reaching maximum when the CNT content is 1 % by weight. The maximum values observed were 1.3 to 1.4 times higher than the basic values. It was also noted that the elongation of composites stays almost invariable when carbon content is below 1 wt. % , due to increase in toughness of composite owing to the highly flexible elastic behaviour of CNT.

Bor et al. [22] used different samples namely un-milled copper, un-milled copper with CNT and milled copper with CNT for processing with planetary ball milling and to analyse the structural and morphological properties. The investigation suggested that the particle sizes of Cu as well as Cu-CNT were increased with increase in rotation speed. The morphologies of particle were drastically changed from aggregated to flatten for high revolutions per minute. On the contrary small changes were observed for the Cu particle and Cu-CNT at low revolution speed. The characterisation revealed that CNTs were weakly joined on copper surface when low speed of rotation was used whereas for high rpm milling , the CNTs were significantly embedded to Cu for the nanocomposites of milled CU with CNT.

Long et al. [23] revealed that the addition of small amount of CNTs increases strength of nano composites which is highly dependent on outside diameters of CNTs. Smaller diameters with same volume percentage resulted in higher composite strength. Possible strengthening mechanisms of CNTs were studied using theoretical models. From theoretical models it is shown that several factors including Volume fraction, model aspect ratio, equivalent plastic strain of transition and material properties of nanotubes. An analytical solution dependent on load bearing effect was developed and it is found that smaller diameters play a key role in reinforcing. By the suitable choice of model parameters material strength of Cu- CNT can be predicted well.

Wei et al. [24] studied the tribological response of copper composites using electric. It was observed that Brinell hardness and thermal conductivity of Cu-CNT composites is always greater than those of Cu-graphite up to 15 % reinforcements.

The coefficient of friction and wear rate decrease with increase in reinforcement amount. For Cu-CNT the dominant wear mechanism was found to be adhesive wear and CNT was found to improve the friction and wear properties of the composite.

2.3 Literature Review on the Wear Modelling

A numbers of wear models are suggested for metals and there are some significant works available in the literature for the wear behaviour prediction of the metallic tribo-pairs. However, due to the complexities involved and ever growing composites with diverse structural heterogeneity, a very few works done till date on modelling and simulation of wear behaviour for composites.

Soderberg et al. [25] applied Archard's wear law in generalised form and Euler's integration for simulating the wear of brake pad assuming dry sliding contact under steady state drag condition. The brake pad interface was modelled as simple as it could be but as complex as necessary. The component is simply modelled such that first surface is the contact region , second is where brake pressure is applied normal to the contact surface and the third joint which keeps the piston coaxial as well as controls the allowed axial displacement. The friction interface materials were modelled as linear elastic materials. The interface was modelled to have asymmetric frictional contact using an augmented Lagrangian algorithm. The connection with calliper was defined as axial displacement. Wear was analysed as a dynamic process and the modelling principle follows wear law at local scale and finds wear depth per unit time as a function of normal load, velocity, material properties and temperature, etc. Wear of the pad was assumed to happen in the direction perpendicular to the rotor surface. They started each step with static analysis wherein it checked the contact pressure at surface of nodes based on the wear during that step and then explicitly integrated so as to calculate total wear. At the end of every step the surface node of pad were shifted inwards depending on the amount of wear at surface so as to avoid convergence problem by preventing the occurrence of open contact between the surfaces. The model was assumed to be valid only till the wear depth is lesser than the element size. The elastic deformation of the material resulted in a symmetric with no uniform pressure variation with high pressure levels directly under the normal load and nearly negligible pressure around the edges.

Thompson et al. [3] proposed a theory which supported that calculation of wear on macro scale is doable for short terms .The approach presented is expected to predict wear on average basis in a manner equivalent with Archard's theory of wear calculation. A constant magnitude load was applied in axial direction of pin. The changes in apparent area of contact with time were assumed to be negligible. The analysis was performed in three load step groups which include displacement to generate the contact, conversion of displacement into load after contact definition, and finally group of load steps. At the end of each sub-step, wear was calculated as an update to the state of strain. The incremental wear strain thus calculated is added to the previously calculated wear strain. It was concluded that a more permanent method needs to be added if wear calculations for larger durations are to be included.

Hegadekatte et al. [26] introduced a global incremental wear model based on Archard's, for computing wear on either pin or disk individually. In this model, they introduced two dimensionless parameters; elastic displacement and a system parameter to determine the relative importance on the computation of wear which is very much essential to decide on when to effectively use a computationally expensive FE based wear simulation method in order to realistically describe the topology after wear. With the help of their suggested model they could see that results for the spherical tipped pin were in good agreement with the experimental results.

Bortoleto et al. [27] correlated analytical formulations using Archard's equation for cylindrical pin wear with stress and contact pressure distributions calculated by finite element analysis for pin-on-disk configuration. It was observed that the mass loss calculated through numerical model was greater than experimental ones due to overestimation of global wear coefficient. Also, friction coefficient was seen directly proportional with load applied which behaviour not in accordance with coulumb's law is.

Rezaei et al. [28] applied adaptive wear simulation which simulated the wear process based on evolving contact conditions. The geometry of the contact varied gradually and resulted into iterative technique in which sliding distance and contact pressure were varied at each iteration. The simulation performs remeshing iterations not only on contact elements but also on their proximity. From the calculated coefficient of wear they suggested that better wear model for more complex contact conditions can be proposed by applying the pressure and sliding velocity. Their results also shown that the wear depth is directly dependent to clearance size.

Yang et al. [29] developed mathematical equations for determining steady state wear coefficients by modifying Archard's wear equation for calculation of the wear coefficient including steady state as well as transient state wear coefficient for aluminium based commercial composites using weight loss data. They also explained the possible causes of wear coefficient variations in the order of tens between transient wear as well as steady state wear regimes.

2.4 Summary of Literature review and Identification of Research gaps

As per the conclusion drawn from literature survey optimum combination of fabrication process and material composition needs further investigation, which requires experimental work as well as mechanistic models of developed composites.

Clustering of reinforcements leads to uneven distribution of the same in the matrix. One of the great challenges in fabricating the Cu-CNT composites is the uniform dispersion of CNTs as CNTs have tremendous surface area, which in turn agglomerates due to van der Waals forces which can lead to worsening of overall properties of the fabricated composite. Since most of the mechanical and thermal properties of the fabricated composite are related to the volume fraction of the reinforcement added, so a homogeneous distribution of reinforcement is essential to obtain the homogeneous properties of the composite. Hence the process of fabrication is can be further reviewed. Different pre-processing such as activators and sonication mediums along with the compaction and sintering procedure needs to be reviewed for the best possible fabrication assuring superior strength, hardness and other desired properties.

There is a little work found in the literature on the tribological characterization using of Cu-CNTs. Especially, there is no significant work found that has been done on modelling of the wear properties and their validation thereof for Cu-CNT composite materials.

Chapter 3 Research Objectives and Methodology

3.1. Introduction

This chapter deals with the formulation of thesis objectives based on the gaps found from the previous chapter and brings in the particulars of the design and analysis of the proposed study. It describes the design of the study based on a selection of number of input parameters, selection of material used for fabrication of composite, the methods and experimental equipment used for fabrication, facilities used for evaluation of properties of the fabricated composites and the parameters which would have helped to achieve the objectives.

3.2. Problem formulation and Setting up Research Objectives

Copper has high thermal conductivity, superior corrosion and oxidation resistance, while CNT enhances strength and wear resistance properties to the matrix. CNT reinforced MMCs are at an emerging research phase. There are several potential applications for these composites, especially the automobile industries. One of such research involving Cu-CNTs can be for their potential tribological applications. The components that are of tribological interests are break shoes, cylinder liners as well as piston rings where high strength and wear resistance as well as good thermal conductivity are some of the desired properties required for the developed materials. Emphasizing tribological behaviour of Cu-CNT within our scope of experimentation we can give attention to the optimization of composite constituents as well as fabrication process parameters to achieve best combination of strength, wear resistance and low coefficient of friction.

Looking at its potential outcome, development of a new material using Cu-CNT composites followed by the detail mechanistic and tribology study requires much needed attention. Accordingly, in the present study following research objectives are defined.

- Fabrication of Cu-CNT composites by powder metallurgy route for the different pre-processing techniques and fabrication cycles.
- Characterization of the fabricated composites.
- Dry tribology study using the fabricated composites.

- Development of wear/penetration model and experimental validation

3.3. Material selection

3.3.1. Matrix

Copper is considered as one of the most commonly used functional and structural metals for engineering applications due to their superior conductivity, low coefficient of thermal expansion, superior corrosion and oxidation resistance. However, there are some drawbacks associated with the pure copper, such as, low yield strength and wear resistance, weak creep resistance and low hardness. Again a lot of properties such as wear resistance can generally be enhanced significantly as compared to monolithic material, by introducing reinforcing phase(s) into the matrix material i.e. making it a composite material.

In the present investigation, Copper metal in powdered form with a mesh size of 325 and 99.5 per cent purity was procured from CDH Fine Chemicals. The details of its overall compositions as mentioned by the supplier data sheet are shown in Table 3.1

Table 3.1: Composition of Metallic Copper by weight percentage

Sb	As	Pb	Fe	Mn	Sn	Cu
0.005%	0.0002%	0.05%	0.01%	0.005%	0.005%	Rest

3.3.2. Reinforcement

It has already been established about the remarkable properties of carbon nanotubes. The increasing interest in utilising it as reinforcement arises from the superior properties of CNTs such as high tensile strength and conductivity, excellent elasticity and chemical inactivity, as compared to the existing graphite fibres. The length to diameter ratios can reach from 100 to 1000 and since their diameter is nanometre sized they also help to retain the isotropy of the base material.

However, the challenge that remains is to implement these properties on macro scale. The strength of composite depends on two factors. Firstly, there should be high degree of load transfer among matrix and nanotubes by adequate bonding between the reinforcements and matrix. Secondly, the homogeneous dispersion of the nanotubes is

a must. If poorly dispersed, nanotubes will fail by separation of agglomerates instead of the failure of nanotubes itself.

For the present work, multi walled CNT with more than 98 carbon basis was purchased from Sigma Aldrich. The specifications of the reinforcement as per the supplier datasheet are given in the following Table 3.2

Table 3.2: Properties of Multi walled Carbon Nanotubes

Carbon content	Form	Outer diameter(nm)	Length(μm)	Metling point($^{\circ}\text{C}$)	Density(g/mL)
>98%	Powder	13-20	15-25	3660	~2.1

3.4. Design of experiments

The selection of number of independent factors to investigate the properties and sliding wear of the composite material is based on the understanding of the process involved as well as the literature survey. In the present study three factors are considered namely ultrasonic agitation energy, volume percentage inclusion of reinforcement with respect to matrix and the sintering temperature which predominantly govern the tribological properties. For present study, the following table describes the combinations of processing parameters selected for composite specimen preparation.

Table 3.3: Processing parameters selected for composite specimen preparation

S.No.	Sonication Energy (% of Maximum Power)	Temperature ($^{\circ}\text{C}$)	CNT (% Vol.)
1	30	750	3
2	30	750	8
3	30	750	12
4	30	850	3
5	30	850	8
6	30	850	12
7	30	950	3
8	30	950	8
9	30	950	12
10	50	750	3
11	50	750	8
12	50	750	12
13	50	850	3
14	50	850	8
15	50	850	12
16	50	950	3
17	50	950	8

18	50	950	12
19	70	750	3
20	70	750	8
21	70	750	12
22	70	850	3
23	70	850	8
24	70	850	12
25	70	950	3
26	70	950	8
27	70	950	12

3.5. Experimental Facility Used For Composite Fabrication and Sample Preparation

3.5.1. Weighing Balance

The digital weighing balance (Mettler Toledo, Greifensee, Switzerland) as shown in Fig. 3.1 was used for weighing a the powders in required ratio of matrix and reinforcement for each sample. This facility is available in Chemical Engineering Department, Thapar University, Patiala. It is a highly accurate and precise measuring device with least count 0.0001 g.



Figure 3.1: Weighing Balance [Chemical Reaction Lab, Thapar University, Patiala]

3.5.2. Ultrasonic agitator

The ultrasonic agitator (Oscar Ultrasonics, Mumbai, India) was used for the sonication of CNT dispersed in acetone for 20 minutes so as to de-agglomerate the CNT clusters created due to Vander-Walls forces of attraction between them. Extremely high pressure, temperature variations and shock waves are involved in this

process. This facility is available in Mechanical Engineering Department, Thapar University.

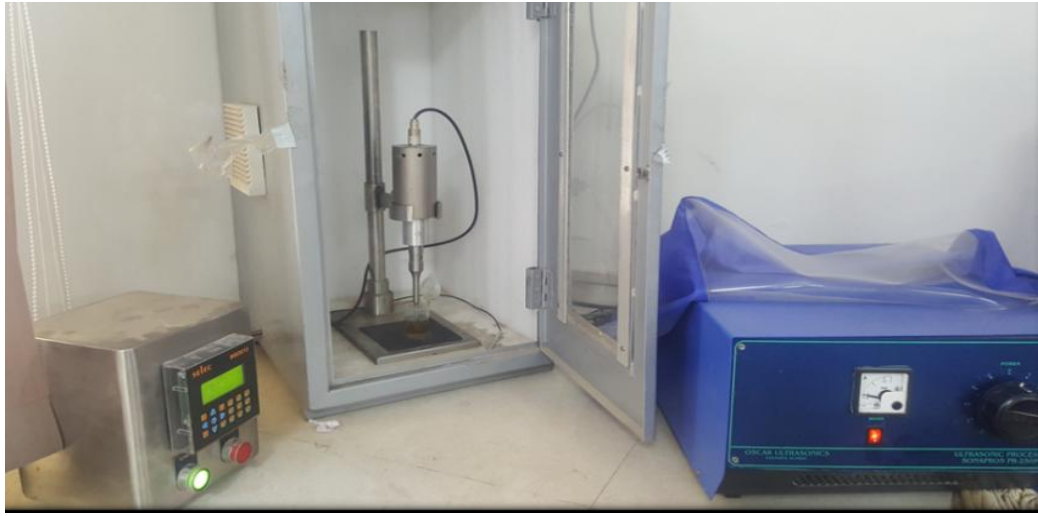


Figure 3.2: Ultrasonicator [Bulk Solids Lab, Thapar University, Patiala]

3.5.3. Molecular level Mixing

After sonication of CNTs the copper powder was dispersed in the CNT-Acetone solution to ensure that the nanotubes wrap around the micro sized copper. The solution was dried overnight to vaporise volatile acetone completely leaving behind the dried mixture of powders.

3.5.4. Ball milling

To further homogenize the mixture, the dried powder was ball milled in batches with a ball to powder ratio of 10:1. Milling was carried out for long durations of 5-6 hours to ensure the proper mixing of the powder. This facility is available in Thapar University, Patiala.

3.5.5. Cold Compression

The mixture powder was put into a cylindrical die made of high speed steel and subjected to a uniaxial cold compression of 10 tonne using manual hydraulic press (Make: PCI Analytics, Mumbai, India) and left for 20 minutes as setting time. This facility is available in School of Physics and Material Sciences, Thapar University, Patiala.



Figure 3.3: Manual Hydraulic Press [SPMS Lab, Thapar University, Patiala]

3.5.6. Sintering

The green samples as a product out of hydraulic press were sintered using a tubular furnace in an inert atmosphere on a heating rate of 3°C per minute for up to 950°C maximum depending on the batch temperature required. The variation in maximum temperature as assigned for every batch was done accordingly. The tubular furnace facility is available in School of Physics and Material Science, Thapar University, Patiala.

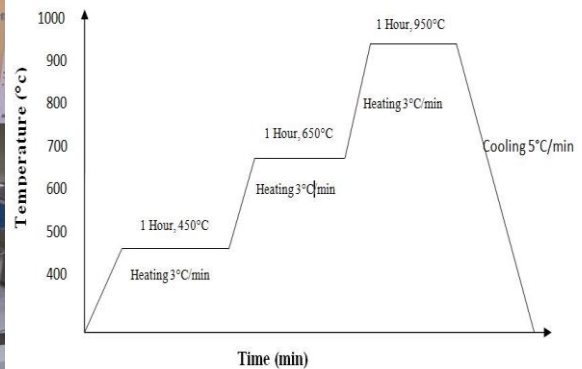


Figure 3.4: (a) Tubular Furnace [Thin Films Lab, Thapar University, Patiala]

(b) Sintering Cycle

3.5.7. Facing

The cylindrically shaped samples were then faced using CNC lathe on the circular faces to ensure the flatness of the pin required for wear testing. Fine cuts of 10 -30

micron were given on each pin so as to avoid undesired surface roughness on faces of pins. This facility is available in Central Workshop , Thapar University, Patiala.



Figure 3.5: Numerically Controlable Lathe Machine [Central Workshop, Thapar University, Patiala]

3.5.8. Disk Polisher

The faced samples were then polished on disk polisher using emery papers successively from 600 to 2000 grit so that proper surface contact is established on pin on disk apparatus. This facility is available in Mechanical Engineering Department, Thapar University, Patiala.

3.6. Experimental Facility Used For Tribology Study

Dry sliding wear tests were performed as per ASTM G99- standards for sliding wear. The material of counter disc was EN31. The counter disc had a diameter range of 20-80 mm and thickness of 8 mm. Both the pin and disc were cleaned by acetone before and after performing the wear test. The pin-on-disk apparatus was used to examine the dry sliding wear characteristics and the coefficient of friction of the hybrid metal matrix composites. The pin which is made up of composite material is rest on a rotating disc under the effect of a dead weight. The tests were conducted under a load of 2.5 kg dead weight and the cumulative wear depth is noted down which appear in form of almost linearly varying graph.

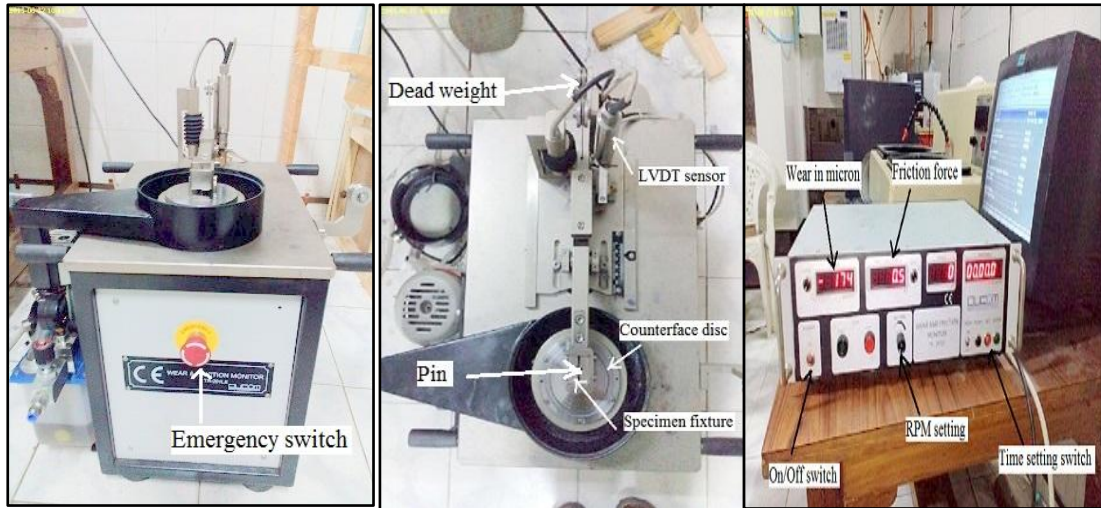


Figure 3.6: Wear testing apparatus[Tribology Lab, Thapar University, Patiala]

3.7. Experimental Facility Used For Mechanical and Metallurgical Investigation

3.7.1. Hardness

Each of the samples were subjected to Vickers hardness tester which is available in Advanced Measurements Laboratory, Thapar University, Patiala. This method comprises of indenting the material using a diamond indenter, which is in the form of a square based pyramid with face angle of 136° . The material is subjected to a load of 1- 100 gm. Full loading is applied for 10-15 seconds. 3 samples from each of the test specimen were taken and their average value was recorded.



Figure 3.7: Micro Hardness Tester [Advanced Measurement Lab, Thapar University, Patiala]

3.7.2. Field Emission Scanning Electron Microscope and EDX

FESEM is made for high resolution imaging for beam sensitive specimens and advanced semi-conductor devices that require stable observation. Basic difference between SEM and FESEM lies between electron behaviour and electron matter interaction. It is a type of electron microscope which produces an image of a specimen by scanning it with a highly focused beam of high energy electrons and produces the information about the sample's surface topography and morphology. In FE-SEM electrons are generated by field emission source. FESEM provides topographical information at very high magnifications (10x to 300,000x). It works on principle that field emission source in the electron gun of a scanning electron microscope produces a narrow beam at low as well as high electron energy which increase its resolution. For present work HITACHI 8020 model was used which is available at SAIF Labs, Panjab University, Chandigarh.



Figure 3.8: FESEM Preprocessing [SAIF Lab, Panjab University, Chandigarh]



Figure 3.9 Laboratory Setup of FESEM [SAIF Lab, Panjab University, Chandigarh]

3.8. Mathematical Calculation of Elastic Properties of Nano composite

Since the sample sizes were very small for determination of elastic properties of the Nano composite using mechanical testing, rather mathematical approach for estimating the required values was followed. The effects of addition of nanotube reinforcements and their agglomeration were investigated theoretically using analytical micromechanics models. The composite is treated as an isotropic material since the nanotubes are dispersed homogeneously throughout the matrix. In the case where agglomeration effect is predicted, the reinforcement clusters are considered as in spherical shape inclusion. The theory used Hill's elastic constants which were dependent on the concentrations of reinforcement(c_r), bulk modulus(k), uniaxial tension modulus(n_r), cross modulus(m_r) and shear modulus(p_r) in direction normal and parallel to the reinforcement of matrix and reinforcement respectively. These are denoted as The mathematical formulas applied for the same are given in Appendix 1.

3.9. Modelling of Wear Depth

When an asperity is pressed against another asperity under some normal load, the deformation is totally elastic in nature and the area in contact will be deformed such that they touch each other over a defined region i.e. a circle. Contact pressures exist over this area which do both the tasks of supporting the applied load and producing the deformations in surfaces.

In the adhesion theory of wear, if multiple asperities are in contact with each other and all of them contribute in production of worn out particle, then the coefficient of wear is assumed to be equal to 1, which is not the case in actual practice and the K values are much lesser than 1. This also leads to the conclusion that indeed many asperity contacts happen without damage .On the surface subjected to repetitive rubbing the contact points should be rubbed multiple times without wear and since plastic deformation is not reversible phenomenon, it can be concluded that some initial deformations may be plastic but majority of the following contacts are elastic in nature.

If an idealised condition of multiple asperity contacts is considered and the deformations considered to be totally elastic in nature, the relationship becomes as shown in eqn (1)

$$\mu = F/W \propto W^{(1-n)} \quad (1)$$

where, the exponent n lies between 0.67 to 1. However, the surfaces having quiet complex topography hold n value extremely close to 1 making the relation as near as direct proportionality.

Multiple contact theory explains that the change in step force is balanced in such a proportion between the new asperities coming in contact due to it, keeping the mean size of contact areas constant i.e. n equals to 1 and average contact pressure over actual contact area remains constant. Also, the surfaces that are prepared by general finishing processes have been studied to have asperity heights relevant to Gaussian form. True area of contact is independent of the apparent area of contact and the maximum levels of stress occur when outermost region of the asperity is pressed to the surface level.

As per the adhesive wear theory given by Archard, considering a single event of rubbing between two asperities, the maximum area in contact $\delta A = \delta W/H$ which is the maximum contribution to true contact area. Also as shown in eqn (2)

$$V/L = KA = K \times (W/H) \quad (2)$$

where, K is the wear coefficient. The above mentioned equation is stated as per fundamental wear theory. For particular calculation of depth of wear, the equation is divided by apparent area of contact which gives us eqn (3)

$$d/L = (K/H) \times (W/A_{APP}) = (K/H) \times P \quad (3)$$

where, P stands for nominal pressure. L in the equation can be expressed as product of sliding velocity and sliding time.

The important controllable material factors for altering the rate of severe metallic wear as suggested by the equation (3) are material hardness, surface hardness, avoidance of welding and compatibility. As reduction of wear is sought after in most of the cases, higher material hardness values prove helpful. Also, surface hardening processes such as carburizing and nitriding for the layer which actually comes in contact with major contact stresses also reduce initial wear. To avoid the mutual welding during the sliding, the use of pure and similar material for

both the surfaces must be avoided as high mutual solubility between metals makes sliding combination incompatible.

In the present study, dry sliding contact of flat pin on disk was simulated using general purpose FEA software package ANSYS. The nanocomposite material properties calculated as discussed were used as input for the material of pin. Since wear is a dynamic process, a generalised form of Archard's law was applied into the software package for calculating the incremental depth of wear. Frictional contact between the interacting surfaces was provided taken from the average value of experiments. Element size of pin was kept of such that expected wear is much lesser than the element size, so as to make the calculations easier. Step size is set to vary between a range so that for every single iteration, first of all the wear is depth is calculated, and then a new iteration begins using updated geometry. The total wear for that time is calculated by adding up the penetration depth data for all time steps which is then compared and validated with experimental data.

In ANSYS Mechanical APDL the loss of material is calculated by repositioning the contact nodes such that the contact surfaces remain in constant touch as in actual experimental conditions. The updated co-ordinates of the new contact nodes are calculated by applying Archard's wear model. The modelling of wear is characterised by type of elements in contact. In practice we have used CONTA173 to define contact surface which is deformable and its sliding between 3 dimensional target surfaces. This element may be used for both general contact or pair based contact. In case of pair based contact which is also required by our model, the target disk surface element is defined by three dimensional element type TARGE170, which is meant for rigid bodies. Surface wear is activated using TB, WEAR command being assigned to contact elements and the wear properties using TBDATA. The material constants needed by the Archard model are defined as input data items through TBDATA command. The implementation involves two stages. In the first stage wear amount is calculated by the wear model, then the geometry is relocated accounting to the wear [2].

The wear direction has been taken opposite to contact normal surface. The successive increment in wear is updated side by side as per the wear so as to maintain continuous sliding condition such that no convergence issues arise due to open contact

surfaces. The contact nodes repositioning may end up in a loss of equilibrium in the model which is tackled by performing additional iterations simultaneously with decreasing step size even more using process of bisection to keep the process quasi static in nature .

Another feature of the model is that solid elements below the element undergoing wear do not experience any stress or strain since wear is a material loss process. Augmented contact algorithm is used with the wear calculation for asymmetric wear i.e. wear on only one side of contact pair.

Chapter 4 Results and Discussion

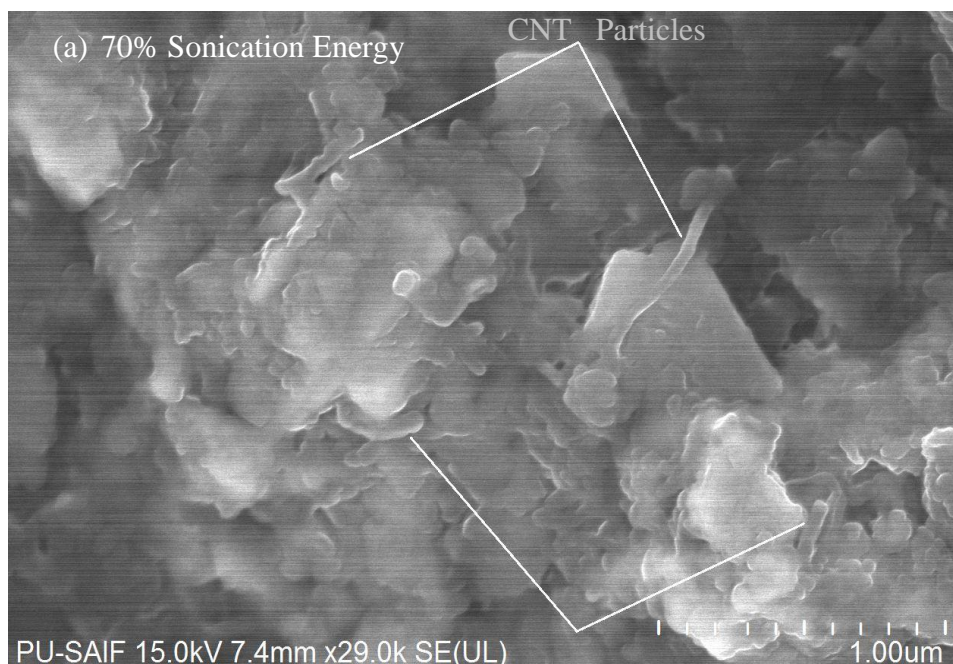
4.1. Introduction

This chapter presents the results and discussion thereof on the mechanical and metallurgical characterizations of the fabricated composites, experimental and simulated results of wear depth.

4.2. Morphological and Metallurgical characterization of fabricated samples

4.2.1. FESEM Micrographs

Field emission microscopy was conducted for the fabricated Nano composites. Since higher hardness values are a favourable characteristic for reduced wear so after conducting the micro hardness tests the specimens showing maximum hardness readings were the subject of interest for morphological characterization. The following figure (Fig. 4.1 a-c) show the FESEM images of the Cu-CNT composite fabricated and sintered at 850°C. These composites are reinforced with 8 per cent CNT each and having hardness value of 120, 118 and 116 VHN. The influence of the reinforcements in hardening effect of matrix was also analysed.



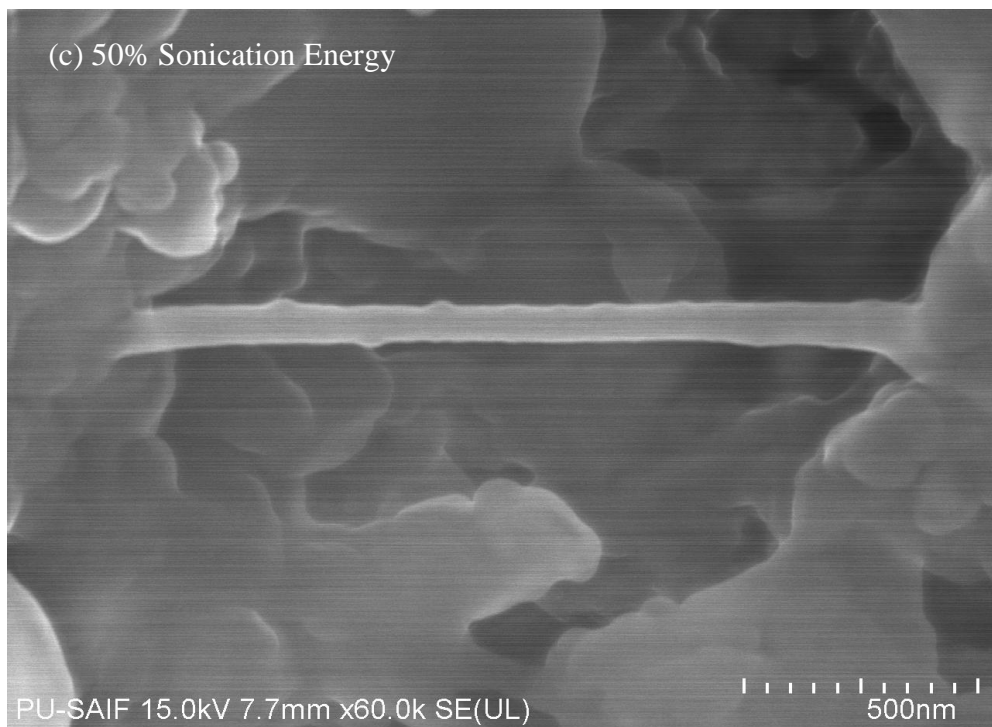
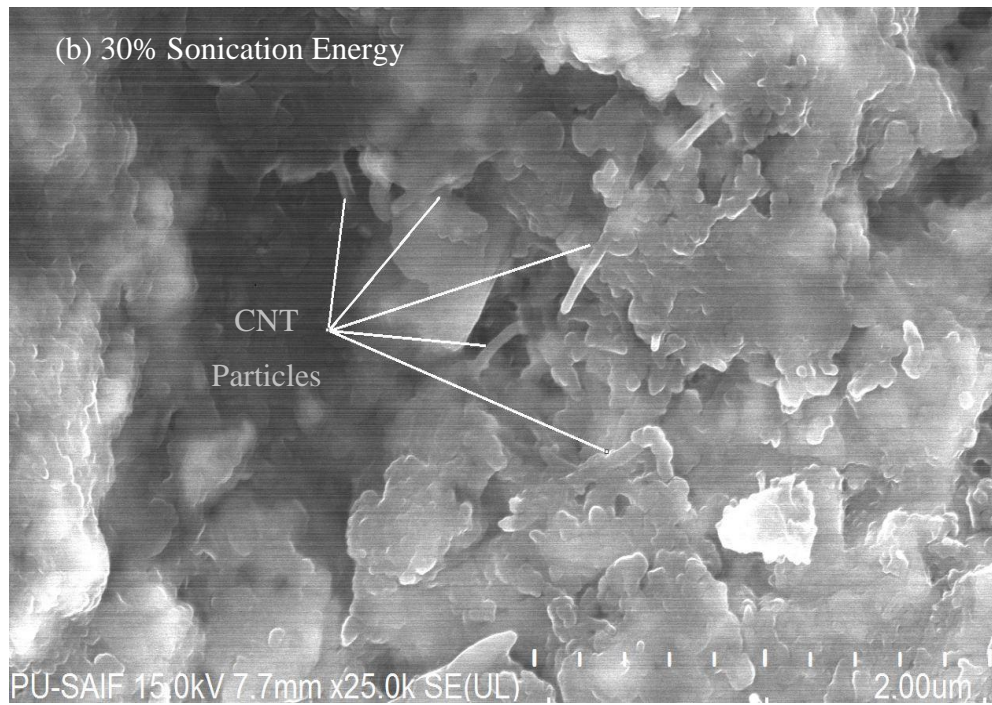


Figure 4.1: SEM Micrographs of specimens with hardness values with CNT as marked (a) 120 VHN (b) 116 VHN (c) 118 VHN

It is evident from the micrographs that there is a fairly homogenous distribution of CNT in the metal matrix which would have provided the raise in bulk

hardness properties of the composite. This may be attributed to the fact that the de-clustering of the agglomerates of the both the particles were taken care of with the use of ultra-sonication and mechanical mixing using ball milling apparatus before the cold compaction of the powder mixture. The homogeneous distribution of secondary phase is required to achieve better mechanical properties and wear resistance.

Moreover, the high aspect ratio along with the elastic properties of CNTs help them to become excellent reinforcement as they provide bridging effect at microscopic level between the cracks which may be present between the matrix molecules as depicted in Fig 4.1 (c) . This adds on to the overall hardness as micro cracks are one of the main reasons for the decrease of the bulk hardness.

4.2.2. Energy Dispersive X-Ray Spectroscopy

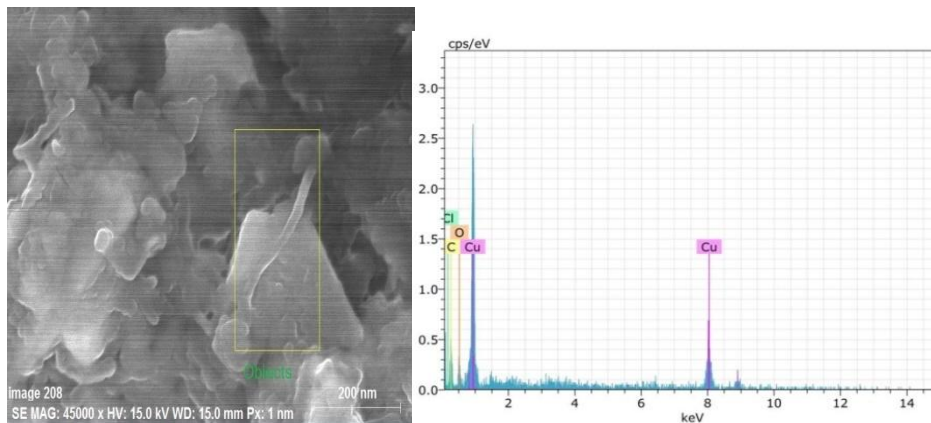


Figure 4.2: EDS Results of specimens with hardness values 120 VHN

Table 4.1 Elemental composition of the fabricated samples with hardness values 120 VHN

Element/Series	Weight %
Copper/K	67.26
Carbon/K	24.41
Oxygen/K	5.80
Chlorine/K	2.03
Total	100

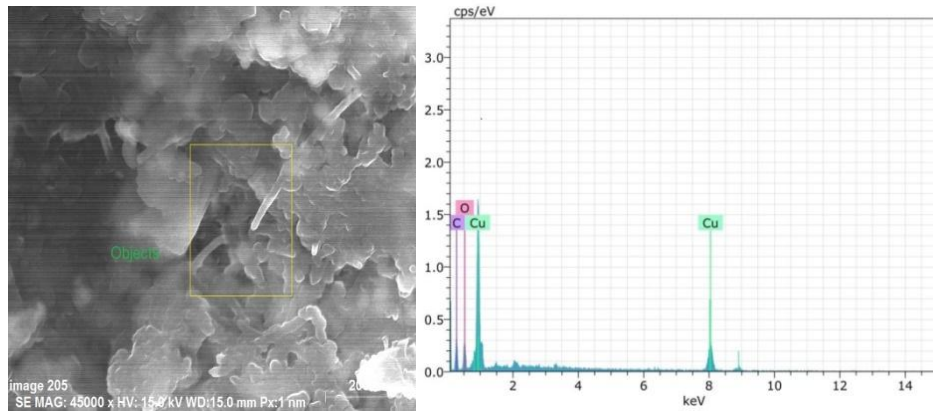


Figure 4.3: EDS Results specimens with hardness values 116 VHN

Table 4.2: Elemental composition of the fabricated samples with hardness values 118 VHN

Element/Series	Weight %
Copper/K	71.12
Carbon/K	20.05
Oxygen/K	9.86
Total	100

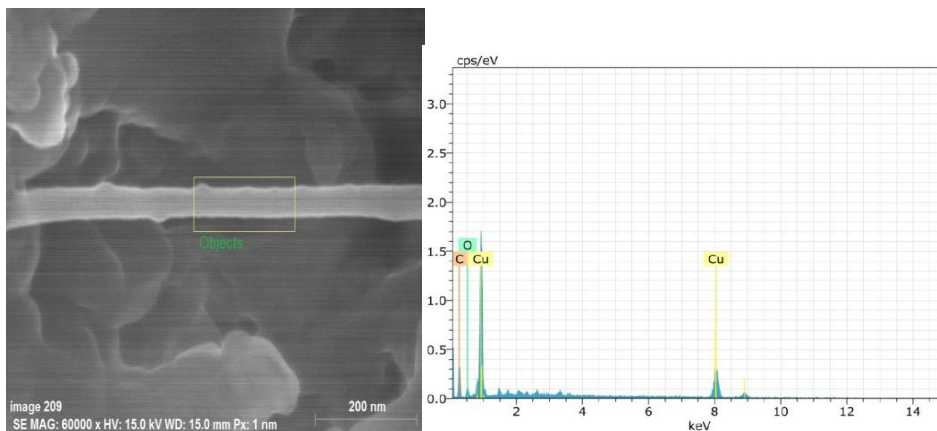


Figure 4.4: EDS Results specimens with hardness values 118 VHN

Table 4.3: Elemental composition of the fabricated samples with hardness values 118 VHN

Element/Series	Weight %
Copper/K	73.26
Carbon/K	24.43
Oxygen/K	4.53
Total	100

Figures 4.2-4.4 and Tables 4.1-4.3 show the EDS taken on the selected areas of the above samples. It is evident from these figures and table that there is significant presence of the CNT in the matrix which was also verified experimentally in the other regions of the samples under investigation. On the other hand, presence of oxygen peak indicates the possibility of oxidation process that occurs during the high temperature sintering. However, it is found not to be as significant as obvious from the elemental composition tables.

4.3. Micro-hardness vs. Wear Depth

Diamond pyramid number is a measure of hardness of material which equals the load value divided by indented area of surface which is calculated by optical measurement of lengths of both the diagonals of indent impression. It uses a pyramid shaped diamond having an included angle of 136° which is pressed on finished components. It works on the principle of ability of resistance to deform plastically from a standard source. This is a widely used scale amongst hardness tests which due to its continuous scale of hardness varying from 5 to 1500 DPN for very soft to very hard materials respectively. It is also known as Vickers Hardness Number (VHN).

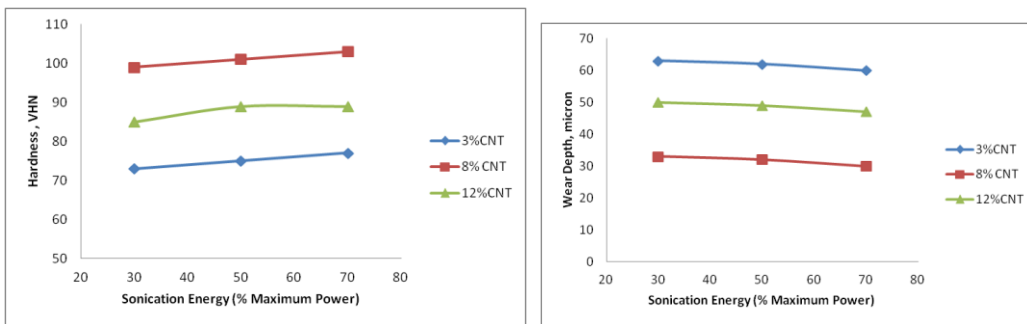
The following table (Table 4.4) shows the hardness (VHN) of various composites. Each data for hardness is obtained by taking average of 5 readings on each sample surface. Table 4.4 also shows the depth of wear tracks formed on the various samples during the dry sliding wear testing. The fabricated composites are used as pin in the dry sliding wear tests.

Table 4.4: Hardness and Wear depth for various composite samples

S.No.	Sonication Energy (% of Maximum Power)	Temperature (°C)	CNT (% Vol.)	Hardness (VHN)	Wear (μm)
1	30	750	3	73	63
2	30	750	8	99	33
3	30	750	12	85	50
4	30	850	3	92	53
5	30	850	8	116	23
6	30	850	12	102	40
7	30	950	3	88	56
8	30	950	8	114	26
9	30	950	12	100	43
10	50	750	3	75	62
11	50	750	8	101	32
12	50	750	12	89	49

13	50	850	3	92	52
14	50	850	8	118	22
15	50	850	12	104	39
16	50	950	3	90	55
17	50	950	8	116	25
18	50	950	12	102	42
19	70	750	3	77	60
20	70	750	8	103	30
21	70	750	12	89	47
22	70	850	3	94	50
23	70	850	8	120	20
24	70	850	12	106	37
25	70	950	3	92	53
26	70	950	8	118	23
27	70	950	12	104	40

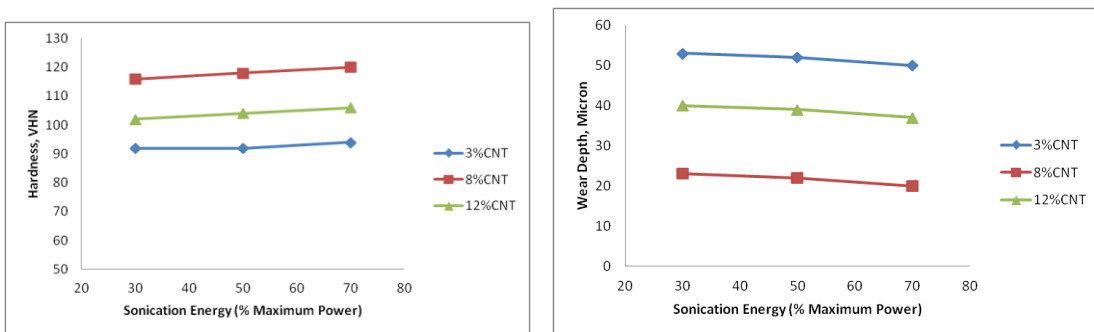
The data from table 4.4 is then analysed and the following comparative plots are generated to show the individual effects on the hardness and wear resistance of the composites.



(a)

(b)

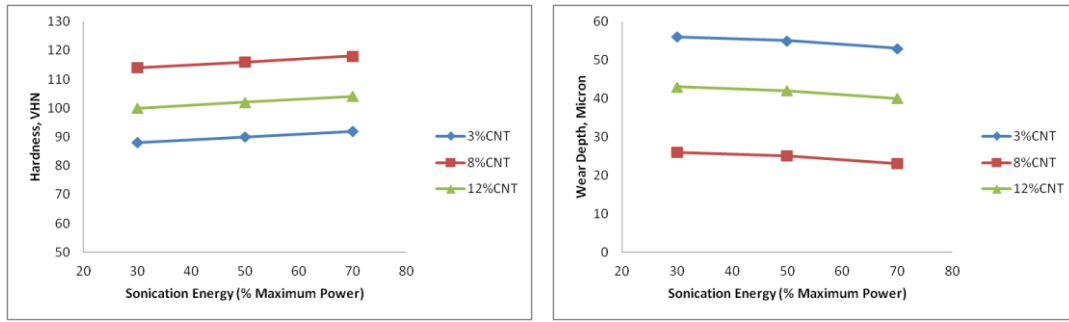
Figure 4.5: Effect of Sonication Energy and % CNT on (a) Microhardness and (b) Wear depth at 750°C



(a)

(b)

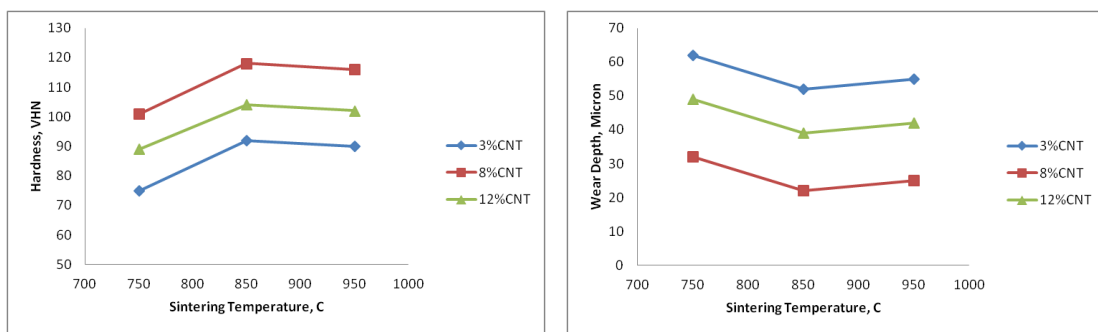
Figure 4.6: Effect of Sonication Energy and % CNT on (a) Microhardness and (b) Wear depth at 850°C



(a)

(b)

Figure 4.7: Effect of Sonication Energy and % CNT on (a) Microhardness and (b) Wear depth at 950°C



(a)

(b)

Figure 4.8: Effect of Sintering Temperature on (a) Microhardness and (b) Wear depth for particles mixing at 50% sonication energy

The analysis of comparative graphs (Figs. 4.5-4.8) clearly depict the dependence of wear depth on the hardness of the pin sample which is again dependent primarily on the amount of CNT content followed by the temperature on which the pin has been sintered. There is an increasing trend in hardness due to the addition of reinforcement upto 8 percent volume. The enhancement of hardness is due to the effect of homogeneous distribution of CNTs in Cu matrix, good bonding at CNT/Cu interfaces and high relative density of nanocomposites. However, at large amount of CNT reinforcement the increase in hardness becomes less significant. This is due to the fact that at increased reinforcement contents the nanotubes start to agglomerate predominantly into the matrix. Due to this agglomeration process the CNT tends to spiral up and entangles themselves as well as with the matrix particles. As a result, the desired properties from CNT into the fabricated composite are greatly affected. Besides, it helps in the formation of voids and porous structure in the resulting composite.

Figure 4.8 shows the effect of sintering temperature on the hardness of the composite. It is seen that as the sintering temperature increase after 850°C, it causes a dip in hardness values possibly due to higher oxidation of trapped air in the pores when subjected to temperatures nearing the melting point of base material (1050°C). The least effective parameter for hardness is noticed to be Sonication Energy in the investigated range, applied for better dispersion of Nano particles.

In all the cases wear depth is found to have inverse relation with the composite hardness. To assess a possible correlation between surface hardness and wear resistance, the following scatter plot is generated with surface hardness of each specimen (Vickers hardness, abscissa axis) against the corresponding wear depth (µm, ordinate axis) obtained from the wear test. This is followed by the regression and correlation tests. A high value of $R^2=0.909$ indicates a strong correlation and an inverse relation between them. Hence, the material's wear decreases as its surface hardness increases

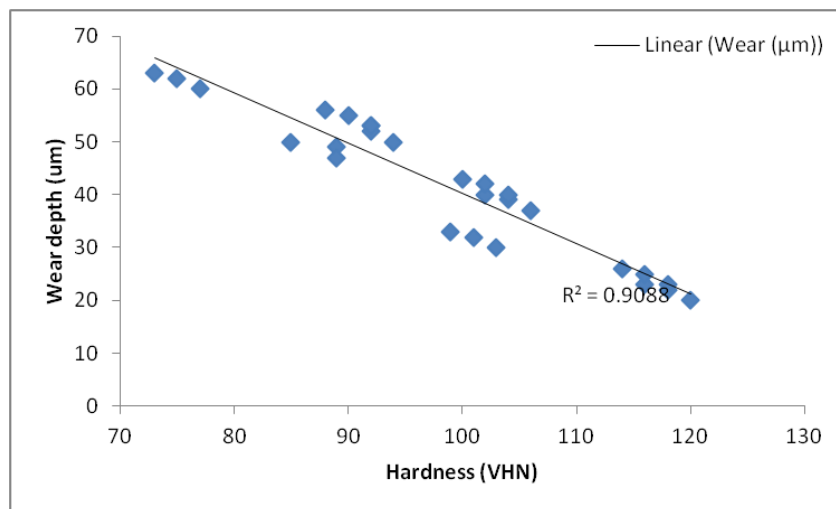


Figure 4.9: Scatterplot of wear depth and Vicker hardness

4.4. Worn Out Pin Surface Analysis

The morphologies of worn out surfaces of pins offer clue to wear mechanisms involved during sliding of the sample against normal load. The wear behaviour with % reinforcement is observed to be similar for various temperatures and predominantly adhesive in nature. Since the composite fabricated at 850°C produced the better result in terms of wear depth so these are taken as the representative samples for further analysis of wear mechanism.

The SEM micrographs of wear tracks of 3 different hardness of composites, fabricated at 850⁰C and tribotested under constant load (24.5 N) are shown in Fig 4.10. From the SEM micrographs, it is evident that all the composites are subjected to mild adhesive wear. The worn surfaces are smooth and ploughing strips are very shallow on the surface and very small damaged spots in the form of craters. The introduction of CNT reinforcing phase to the copper matrix reduces the contact area between the pure copper and the counter disc. This reduction in the effective contact area between the copper matrix and the disc leads to the improvement of the wear resistance. However, this phenomena is effective only if the reinforced amount is suitably optimized. In the present case, from the SEM micrographs, it is evident that composite with 3%CNT (Fig. 4.10a) is unable to reduce adhesive wear loss significantly, since it can not envelope the copper matrix by providing sufficient high load bearing asperities contributed from CNTs. Since the pin material is very soft as compared to counter surface, as a result the hard asperities from the counter surface may plough or form adhesive weld with the pin surface and results in large adhesive wear grooves.

In the case of composite with 8% CNT (Fig. 4.10b), it was found that the wear loss of the composite is lower than that of the composite with 3% and 12% CNT (Fig. 4.10a,c). It may be attributed to the fact of hardness enhancement as well as uniform distribution of CNTs in the matrix of copper, providing the better contact surface against the sliding disk. The wear resistance is found to be high since the hardness of the sample also increases due to the better distribution and high strength of the reinforcement agents. The size and numbers of wear grooves gets reduced in the pin worn out surface. The dispersed CNTs in Cu-matrix nano-composite gives significantly enhanced wear resistance by retarding the peeling of Cu grains during sliding wear process.

However, if the reinforcement content is further increased wear resistance is found to be decreased in inverse proportion to hardness of material. There is the decrease in hardness due to clustering of reinforcement. The hard asperities from the counter surface plough the composite surface and the weak bonded and clustered CNTs are thrown out from the matrix, resulting in the some large sizes of the craters distributed on the surface of the worn out composite pins.

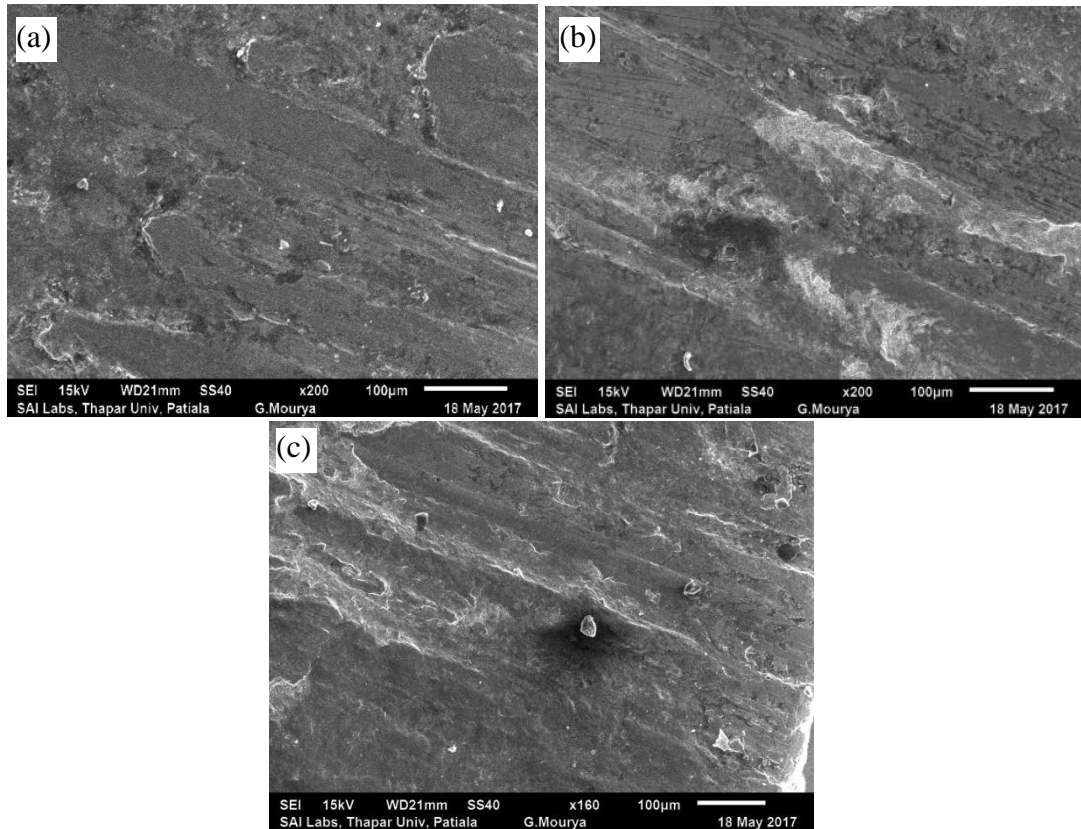


Figure 4.10: Pins Worn Surface (a) 3% CNT (b) 8% CNT (c) 12% CNT

The other factor which is influence the improved wear resistance of the Cu-CNT composite is the formation of graphite layers produced in the presence of CNT reinforcement phase and which are released upon application of shear stresses induced by the wear process. This leads to the reduction in the friction coefficient and improves the wear resistance. The abundance of carbon from EDS analysis on the pin wear tracks as shown in the Table 4.5 and 4.6 confirms our claim.

Table 4.5: Elemental composition of Pin Worn Surface (8% CNT)

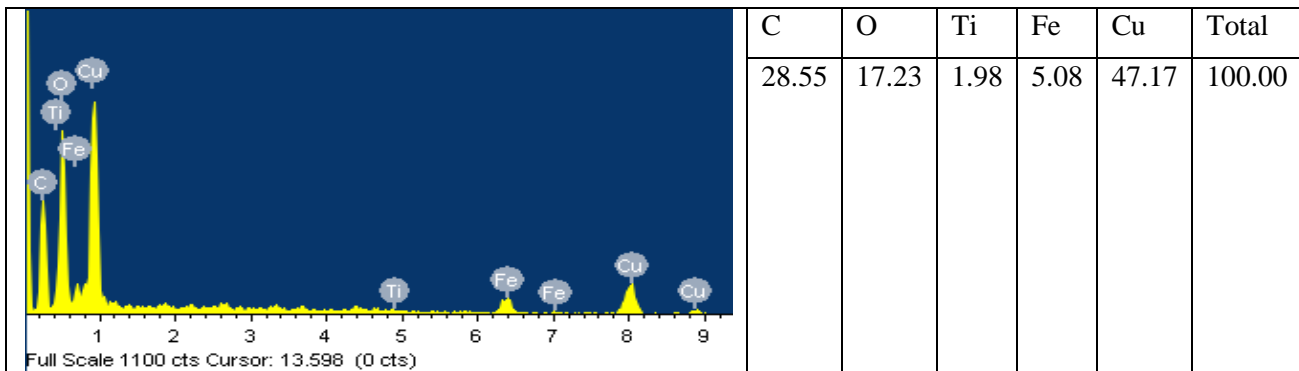
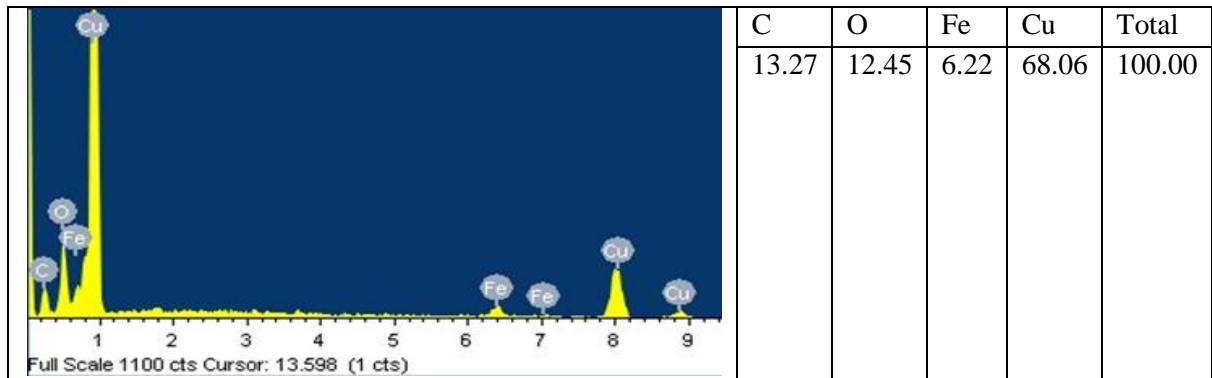


Table 4.6: Elemental composition of Pin Worn Surface (3% CNT)



Again, the enhanced sliding wear resistance of the composites may be due to the strain hardening of the matrix due to the differential thermal expansion of matrix and reinforcement, delamination of mechanically mixed layer consisting of Fe and copper and the sliding resistance offered by the oxide layer. The elemental analysis of the worn out pins suggest the presence of small amount of Fe elements on its surface along with the mild increase in oxygen content in both the specimens which suggests that due to rise in temperature during wear testing, the surface oxidation must have taken place. The trapped iron suggests that mild wear of harder counter disk material also occurs however it is not as significant as pin wear.

4.5. Disc Wear Track Analysis

For the further investigation on the wear mechanism following the wear test, the counter surface disk was taken for SEM and EDS elemental analysis. As observed from the graphs of elemental analysis of the wear tracks on the counter disk surface, transfer of a very small amount of copper and carbon on the surface of wear tracks has been found. The softer powdered materials from composite were observed to be deposited on disc surface forming an impression of wear track. However, wear debris was observed to be powdered particles of metallic copper.

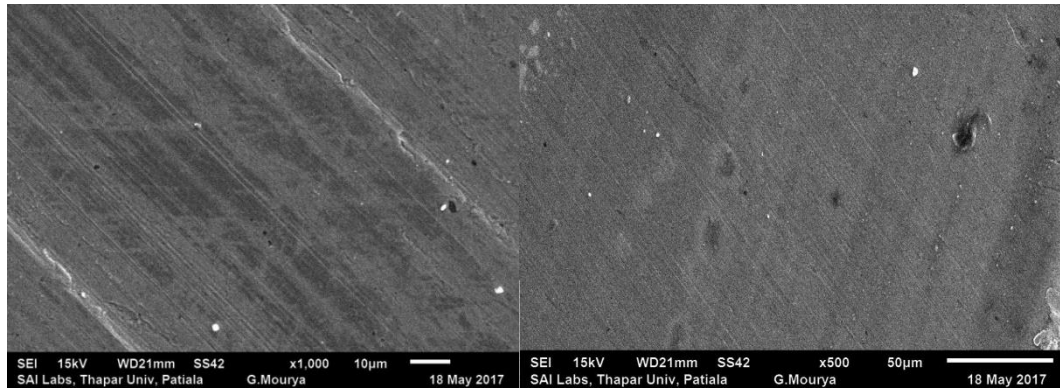
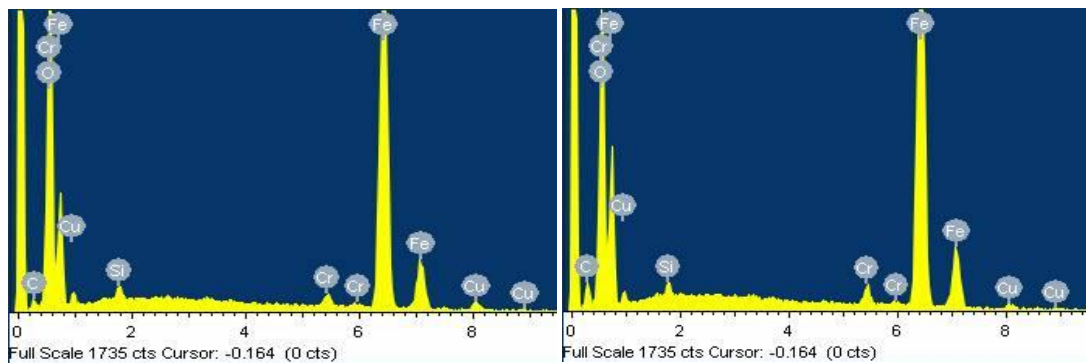


Figure 4.11: Wear track on the counter disc

Table 4.7: EDS results of counter disk subjected to pins with hardness values (a)120VHN (b)118 VHN



The gradual increase in wear depth as shown in tribometer data suggested that there was not much reverse transferring of copper from debris layer to the pin and no permanent tribolayer was observed during the initial phase of the tribotest. On repetitive rotations, the accumulated particles of copper formed aggregates followed by their removal from track to the nearby surface. Since the process is in dynamic equilibrium, the pace of wearing out proportional to transfer rate of composite from pin to disk surface. After achieving the equilibrium surface conditions due to completion of running in period the surfaces become relatively smoother and mild wear occurs causing particle removal in the form of finely divided metal followed by possible oxidation.

4.6. Finite Element Simulation of Wear

In this section, an attempt is made to FE simulation of dry sliding wear of copper composite. For the purpose of simulation, a replica of actual pin on disk setup was created in general purpose ANSYS software. The element body sizing was assigned

to the model resulting in formation of 6943 elements and 16239 nodes which formed a meshed structure as shown Fig (4.12) below.

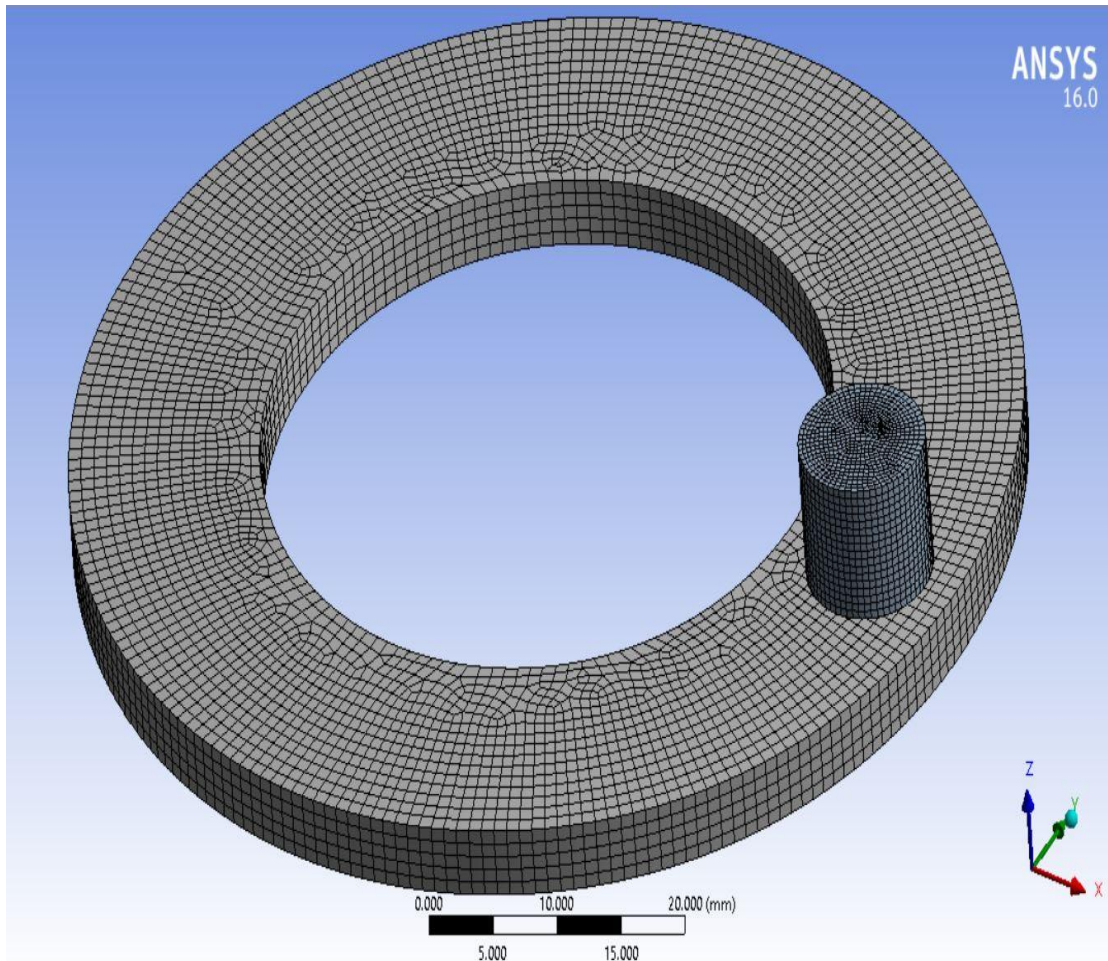
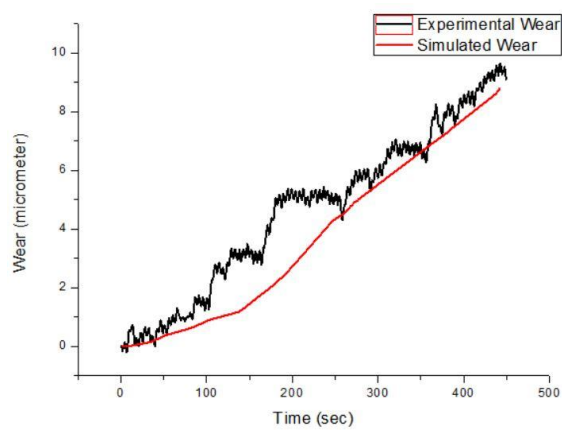


Figure 4.12: Mesh Generation for Pin on Disk apparatus



(a)

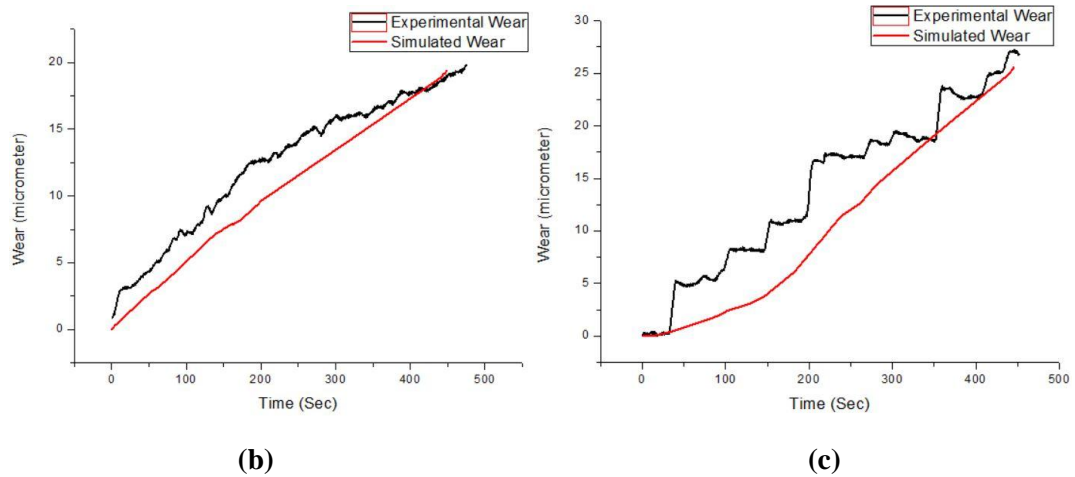


Figure 4.13: Simulated and experimental wear depth obtained for specimens (a)120 VHN (b)92 VHN (c)73 VHN

It is a commonly observed phenomena that even if the wear is supposed to increase linearly, it often shows curvilinear start indicating higher wear rate in the starting phase of wearing out. This time is termed as running in period or transient wear after completing which the wear rate is quiet stable and is termed as steady state wear. For most of the experimental wear tests conducted the running in time for Copper-CNT composite was observed to be in the range of 150-180 seconds after which the slope of wear depth graph decreased to some extent and remain nearly stable till the 1200 seconds of tests conducted. Fig 4.15 shows one of the experimental wear depth graph depicting the aforesaid phenomenon.

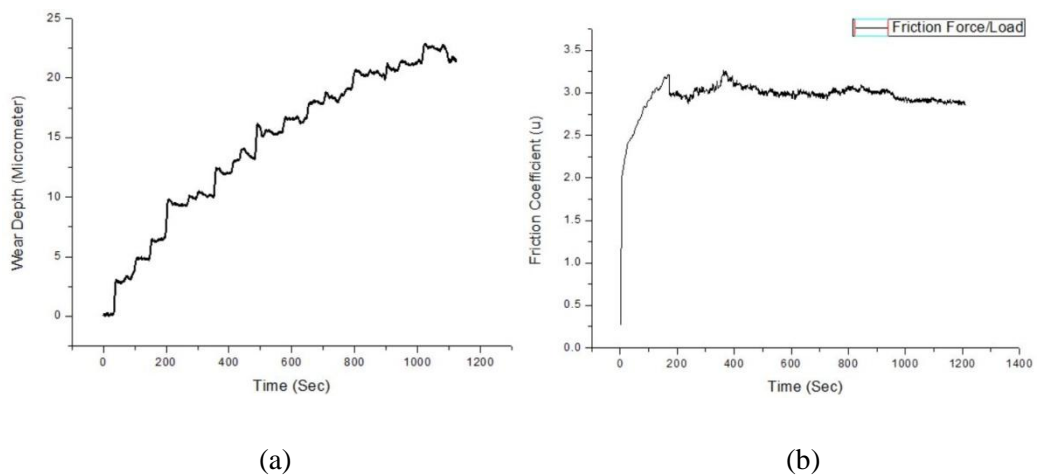


Figure 4.14: (a)Typical wear Depth plot depicting variation in slope with time (b) Typical friction plot

Generalised Archard’s wear model was inserted in ANSYS Mechanical APDL (Ansys Parametric Design Language) using the known experimental inputs such as hardness and coefficient of friction (in the present case it is 0.3) and the

coefficient of wear was varied in the ranges of order 10^{-4} to 10^{-6} so as to achieve most accurate K value satisfying the experimental results. It was then observed that $1.3-1.4 \times 10^{-5}$ was the suitable range where the experimental as well as simulated results shows the similar behaviour. Based on this simulated K to confirm its validity for the present composite another set of experimental and simulated wear penetration data is then collected and compared by giving input K value as 1.4×10^{-5} and the results are shown in the following Fig. 4.15

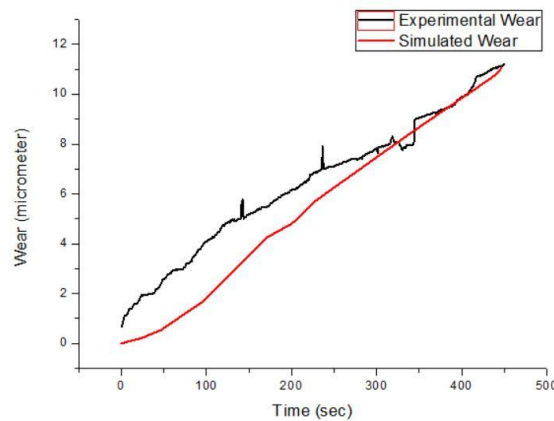


Figure 4.15: Simulated and experimental wear depth obtained for hardness 116 VHN and $K=1.4 \times 10^{-5}$

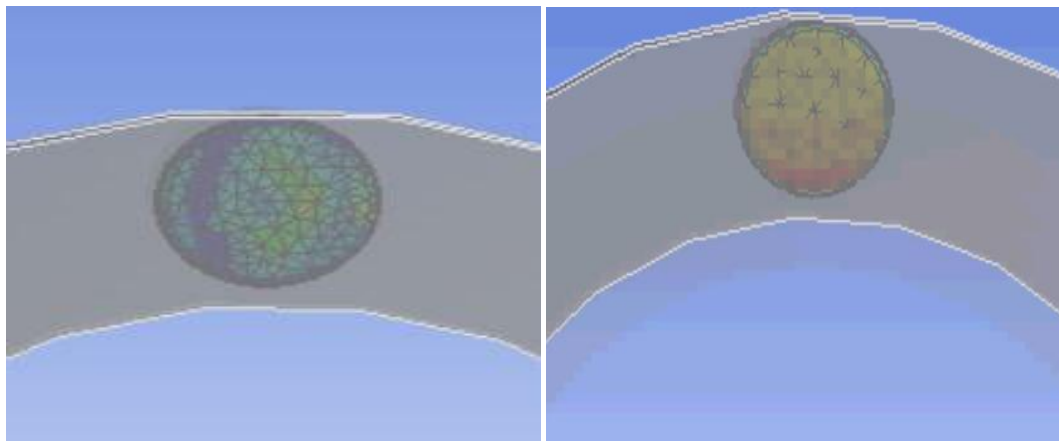


Figure 4.16: Surface profile of Composite Pin for wear simulation (a) 10 sec after start (b) After 440 Sec

The images for simulated surface profile of composite pin show the regions where maximum and minimum penetration is occurring for the specimen (116 VHN). Blue colour signifies minimum penetration and red signifies maximum. During the start of the simulation, some portion of the pin showed variable penetration which gets uniform at the end of simulation. Thus the conformal test data result validated the

predicted K value. This is true as far as finding the net wear rate was concerned i.e. by minimising the concern for transient wear phase. Also, the simulated depth data results were close to linear correlation with time.

4.7. Summary

From the above mentioned results followed by their discussion, it can be summarised that enhancement of tribological properties of Cu-CNT composite material is a multivariable problem depending on the fabrication route followed as well as the reinforcement content which is homogenously distributed within the matrix. Optimization of such parameters is important for achieving the desired results such as reduced wear rate from the tribology point of view. Furthermore, non-destructive testing of newly developing materials is possible using the mathematical equations in combination with experimental inputs such as coefficient of wear of Cu-CNT material was in our case.

Chapter 5 Conclusion

5.1. Conclusion

The CNT particle reinforced copper matrix composite is successfully prepared by powder metallurgy technique. These are then subjected to mechanical and wear characterization. The wear behaviour of the fabricated composites is then simulated using ANSYS. The present research work lead to the following conclusions:

- Nanocomposites fabricated by inserting the CNTs into the copper matrix showed the tangible hardness enhancement. The enhancement in the mechanical properties is observed as the volume percentage of reinforcement is increased up to a certain extent. As compared to base Copper, hardness is found to be increased by approximately 100%.
- The sintering temperature at which the fusion between two materials take place plays a significant role in determining the mechanical properties of the composite.
- The observed decrease in hardness of composite after 850°C is possibly due to oxidation of the metal with the air trapped in the pores. The increased fluidity of metal particle after achieving a certain temperature is also a possible reason for decreased hardness.
- The optimum parameters for fabrication Cu-CNT composite in the present research is found to be 850°C sintering temperature and 8% CNT reinforcement.
- The composites containing higher volume of CNT reinforcement tend to have increased wear resistance.
- The sonication energy for dispersion of powders seem to have insignificant influence on the resultant mechanical properties and wear resistance of the fabricated composite.
- The amount of wear of the fabricated composite is found to have strong inverse correlation with the hardness of the material.
- From the FE simulation, the wear coefficient of the composites under investigation has been estimated in the range of $(1.3-1.4) \times 10^{-5}$.

5.2. Recommendation for future works

A major simplification in the wear routine presented is that it only simulates wear of the pin. A natural next step is to expand the simulation routine to consider wear at both contact surfaces. Another simplification in the present FE model is that the disk is represented as rigid body. If wear of the disk is to be included in the model, it would also be interesting to study how elastic deformation of the disk surface affects the contact conditions. This design question will require an alternative FE representation of the rotor, modelling it as a deformable body. This will increase the complexity of the model by adding additional degrees of freedom, but may produce important information about the system.

References

- [1] J. F. Archard, "Wear Theory and Mechanisms" *Wear Control Handbook* . pp. 35–80, 1980.
- [2] J. Gubicza "Theory Reference for the Mechanical APDL and Mechanical Applications," vol. 3304, no. April, pp. 724–746, 2009.
- [3] J. M. Thompson and M. K. Thompson, "A Proposal for the Calculation of Wear Mechanisms of Wear," *Int. ANSYS Conf.*, pp. 1–14, 2002.
- [4] O. Breuer and U. Sundararaj, "Big returns from small fibers: A review of polymer/carbon nanotube composites," *Polym. Compos.*, vol. 25, no. 6, pp. 630–645, 2004.
- [5] J. W. Kaczmar, K. Pietrzak, and W. Wlosinski, "The Production and Application of Metal Matrix Composite Materials," *J. Mater. Process. Technol.*, vol. 106, no. 1–3, pp. 58–67, 2000.
- [6] M. Yu, "Strength and Breaking Mechanism of Multiwalled Carbon Nanotubes Under Tensile Load," *Science (80-.)*, vol. 287, no. 5453, pp. 637–640, 2000.
- [7] K. Rajkumar and S. Aravindan, "Tribological performance of microwave sintered copperTiCgraphite hybrid composites," *Tribol. Int.*, vol. 44, no. 4, pp. 347–358, 2011.
- [8] V. T. Pham *et al.*, "The effect of sintering temperature on the mechanical properties of a Cu/CNT nanocomposite prepared via a powder metallurgy method," *Adv. Nat. Sci. Nanosci. Nanotechnol.*, vol. 2, no. 1, p. 15006, 2011.
- [9] M. B. Vishlaghi and A. Ataie, "Role of Intensive Milling on Microstructural and Physical Properties of Cu 80 Fe 20 / 10CNT Nano-Composite," vol. 47, no. 1, pp. 37–42, 2014.
- [10] P. Bakhshaei, A. Ataie, and H. Abdizadeh, "Effect of CNT Addition on the Characteristics of Cu-Ni / CNT Nanocomposite," *J. Nanostructures*, vol. 3, no. 2013, pp. 403–409, 2014.
- [11] H. Li *et al.*, "Strong and ductile nanostructured Cu-carbon nanotube composite," *Appl.*

- Phys. Lett.*, vol. 95, no. 7, pp. 1–4, 2009.
- [12] S. R. Dong, J. P. Tu, and X. B. Zhang, “An investigation of the sliding wear behavior of Cu-matrix composite reinforced by carbon nanotubes,” *Mater. Sci. Eng. A*, vol. 313, no. 1–2, pp. 83–87, 2001.
- [13] K. Chu, C. Jia, L. Jiang, and W. Li, “Improvement of interface and mechanical properties in carbon nanotube reinforced Cu–Cr matrix composites,” *Mater. Des.*, vol. 45, pp. 407–411, 2013.
- [14] D.-L. Shi, X.-Q. Feng, Y. Y. Huang, K.-C. Hwang, and H. Gao, “The Effect of Nanotube Waviness and Agglomeration on the Elastic Property of Carbon Nanotube-Reinforced Composites,” *J. Eng. Mater. Technol.*, vol. 126, no. 3, p. 250, 2004.
- [15] L. Y. Wang *et al.*, “Friction and wear behavior of electroless Ni-based CNT composite coatings,” *Wear*, vol. 254, no. 12, pp. 1289–1293, 2003.
- [16] S. M. Uddin *et al.*, “Effect of size and shape of metal particles to improve hardness and electrical properties of carbon nanotube reinforced copper and copper alloy composites,” *Compos. Sci. Technol.*, vol. 70, no. 16, pp. 2253–2257, 2010.
- [17] S. J. Yoo, S. H. Han, and W. J. Kim, “A combination of ball milling and high-ratio differential speed rolling for synthesizing carbon nanotube/copper composites,” *Carbon N. Y.*, vol. 61, pp. 487–500, 2013.
- [18] K. T. Kim, S. Il Cha, and S. H. Hong, “Hardness and wear resistance of carbon nanotube reinforced Cu matrix nanocomposites,” *Mater. Sci. Eng. A*, vol. 448–451, pp. 46–50, 2007.
- [19] P. Jenei, E. Y. Yoon, J. Gubicza, H. S. Kim, J. L. Lábár, and T. Ungár, “Microstructure and hardness of copper-carbon nanotube composites consolidated by High Pressure Torsion,” *Mater. Sci. Eng. A*, vol. 528, no. 13–14, pp. 4690–4695, 2011.
- [20] S. A. Alidokht, A. Abdollah-zadeh, and H. Assadi, “Effect of applied load on the dry sliding wear behaviour and the subsurface deformation on hybrid metal matrix composite,” *Wear*, vol. 305, no. 1–2, pp. 291–298, 2013.
- [21] C. F. Deng, D. Z. Wang, X. X. Zhang, and A. B. Li, “Processing and properties of carbon nanotubes reinforced aluminum composites,” *Mater. Sci. Eng. A*, vol. 444, no.

- 1–2, pp. 138–145, 2007.
- [22] A. Bor, B. Ichinkhorloo, B. Uyanga, J. Lee, and H. Choi, “Cu/CNT nanocomposite fabrication with different raw material properties using a planetary ball milling process,” *Powder Technol.*, 2015.
- [23] X. Long, Y. Bai, M. Algarni, Y. Choi, and Q. Chen, “Study on the strengthening mechanisms of Cu/CNT nano-composites,” *Mater. Sci. Eng. A*, vol. 645, pp. 347–356, 2015.
- [24] A. Söderberg and S. Andersson, “Simulation of wear and contact pressure distribution at the pad-to-rotor interface in a disc brake using general purpose finite element analysis software,” *Wear*, vol. 267, no. 12, pp. 2243–2251, 2009.
- [25] V. Hegadekatte, N. Huber, and O. Kraft, “Modeling and simulation of wear in a pin on disc tribometer,” *Tribol. Lett.*, vol. 24, no. 1, pp. 51–60, 2006.
- [26] E. M. Bortoleto *et al.*, “Experimental and numerical analysis of dry contact in the pin on disc test,” *Wear*, vol. 301, no. 1–2, pp. 19–26, 2013.
- [27] A. Rezaei, W. Van Paepegem, P. De Baets, W. Ost, and J. Degrieck, “Adaptive finite element simulation of wear evolution in radial sliding bearings,” *Wear*, vol. 296, no. 1–2, pp. 660–671, 2012.
- [28] L. J. Yang, “Wear coefficient equation for aluminium-based matrix composites against steel disc,” vol. 255, pp. 579–592, 2003.

Appendix A: Formulae used for the calculation of various elastic constants

$$\alpha_r = (3*(K_m + G_m) + k_r - l_r) / (3*(G_m + k_r)) \quad A1$$

$$\beta_r = (0.2*((4*G_m + 2*k_r + l_r) / (3*(G_m + k_r))) + ((4*G_m) / (G_m + p_r)) + 2*((G_m*(3*K_m + G_m)) + (G_m*(3*K_m + 7*G_m))) / ((G_m*(3*K_m + G_m)) + (m_r*(3*K_m + 7*G_m)))) \quad A2$$

$$\delta_r = 0.333*(n_r + (2*l_r) + ((2*k_r + l_r)*(3*K_m + 2*G_m - l_r)) / (G_m + k_r)) \quad A3$$

$$\eta_r = 0.2*((0.667*(n_r - l_r) + ((8*G_m*p_r) / (G_m + p_r)) + ((2*(k_r - l_r)*(2*G_m + l_r)) / (3*(G_m + k_r))) + (8*m_r*G_m*(3*K_m + 4*G_m)) / (3*K_m*(m_r + G_m) + (G_m*(7*m_r + G_m)))) \quad A4$$

$$K = K_m + (c_r*(\delta_r - 3*K_m*\alpha_r) / (2*(c_m + c_r*\beta_r))) \quad A5$$

$$G = G_m + (c_r*(\eta_r - 2*G_m*\beta_r) / (2*(c_m + c_r*\beta_r))) \quad A6$$